Transcriptome Landscape of Human Oocytes and Granulosa Cells Throughout Folliculogenesis

Yaoyao Zhang [1,2,3,8], Zhiqiang Yan[1,5,8], Qingyuan Qin[1,3,4,8], Vicki Nisenblat[1,4], Yang Yu[1,2,3], Tianren Wang[1,2,3], Cuiling Lu[1,2,3], Ming Yang[1,2,3], Shuo Yang[1,2], Ying Yao[5], Xiaohui Zhu[1,3,4], Xi Xia[1,2,3], Yujiao Dang[1,3,4], Yixin Ren[1,3,4], Peng Yuan[1,3,4], Rong Li[1,2,3], Ping Liu[1,2,3], Hongyan Guo[5], Jinsong Han[5], Haojie He[5], Yu Wu[5], Meng Li[5], Kun Zhang[5], Yiting Wang[5], Jie Qiao[1,2,3,5,6,9*], Jie Yan[1,2,3*], Liying Yan[1,2,3*]

[1] Center for Reproductive Medicine, Department of Obstetrics and Gynecology, Peking University Third Hospital, No.49 North HuaYuan Road, HaiDian District, Beijing 100191, China;

[2] National Clinical Center for Obstetrics and Gynecology, Beijing 100191, China;

[3] Key Laboratory of Assisted Reproduction, Ministry of Education, Beijing 100191, China;

[4] Beijing Key Laboratory of Reproductive Endocrinology and Assisted Reproduction, Beijing 100191, China;

[5] Peking-Tsinghua Center for Life Sciences, Peking University, Beijing 100871, China

[6] Department of Obstetrics and Gynecology, Peking University Third Hospital, No.49 North HuaYuan Road, HaiDian District, Beijing 100191, China;

[7] Beijing Advanced Innovation Center for Genomics (ICG), Peking University, Beijing 100871, China;

[8] Co-first author

[9] Lead Contact

[*] Corresponding: jie.qiao@263.net (J.Q.), yanjiebjmu@bjmu.edu.cn (J.Y.), yanliyingkind@aliyun.com (L.Y.).

SUMMARY

Folliculogenesis is a highly regulated process that involves bidirectional interactions of the oocytes and surrounding granulosa cells (GCs). Little is unknown, however, about the transcriptomic profiles of human oocytes and GCs throughout folliculogenesis. Here we performed a high resolution RNA-Seq of human oocytes and GCs at each follicular stage, which revealed unique transcriptional profiles, stage-specific signature genes, oocyte- and GC-derived genes that reflect ovarian reserve. We identified reciprocal cell-to-cell interactions between oocytes and GCs, including NOTCH, TGF-β signaling and gap junctions and determined the expression patterns of maternal-effect genes involved in folliculogenesis and early embryogenesis. Finally, we demonstrated robust differences between human and mice oocyte transcriptomes. This is the first comprehensive overview of the transcriptomic signatures governing the stepwise human folliculogenesis in-vivo that provides a valuable resource for basic and translational research in human reproductive biology.

INTRODUCTION

Human folliculogenesis is a remarkably complex, well-orchestrated process that relies on a synchronization between oocyte maturation and proliferation of the neighboring granulosa cells (GCs) [1,2]. Follicle growth and oocyte maturation are associated with dynamic transcriptional events in both oocyte and GC compartments of the follicle, featured by high transcriptional activity of growing follicles post recruitment and transcriptional silencing of mature oocytes [3]. Despite the impressive body of data produced in recent years on oocyte biology, many questions regarding the key differentiation events occurring during folliculogenesis in humans remain unanswered Oocyte-GCs bidirectional communications via signal transduction or direct cell-to-cell contact provide molecular and structural basis for effective oocyte-GC crosstalk required for adequate follicular development. It is poorly understood, however, what initiates [4] the communication between human follicle compartments and how this interaction is regulated and maintained.

Genes that accumulate in oocytes during maturation and influence early embryonic development are referred to as maternal-effect genes[5]. The events associated with maternal-effect genes and the process of maternal-to-zygotic transition have been studied in animal models [6], albeit the expression pattern and the role of these genes during oocyte development in humans remain unclear. In women, reproductive potential and reproductive lifespan depend on the follicle number available for fertilization and the rate of follicular loss during reproductive years, both of which

63 determine ovarian reserve [7]. Even though the levels of tests such asanti-Mullerian
64 hormone and follicle stimulating hormone (FSH), and the antral follicle count
65 measured by transvaginal ultrasound has been widely used to predict ovarian reserve,
66 the universally accepted markers that accurately predict fertility potential and ovarian
67 reserve are still lacking [8-10].

68 Till now, most data on follicular transcriptome are derived from the studies on animal
69 models due to restricted availability of human follicles for research. While animal
70 studies have advanced our understanding of ovarian biology, expression patterns of
71 oocyte-specific genes are known to display considerable interspecies variations [11]. In
72 humans, transcriptomic studies of ovarian follicle rely on evaluations of the oocytes at
73 limited stages of development or on analysis of unseparated follicle compartments [12-14],
74 which undermines the applicability of the findings to understanding of a coherent
75 whole of folliculogenesis. Application of single-cell RNA sequencing (scRNA-Seq)
76 and other high resolution sequencing techniques allows an unbiased evaluation of cells
77 of any size and efficient amplification of low-abundant transcripts, which makes these
78 methods a powerful tool in studying the biological process of interest[15]. Therefore,
79 characterizing human oocyte and GC transcriptome during different stages of
80 development at high resolution is key to understanding the events that coordinate
81 human oocyte maturation and follicle growth, which in turn is expected to provide
82 remarkable opportunities for developing novel diagnostic and therapeutic approaches
83 to improve fertility.

This work aimed at analyzing the gene expression patterns throughout folliculogenesis by exploring the transcriptome of human oocytes and GCs at five key stages of follicular development in-vivo, from primordial to preovulatory stage. Using scRNA-Seq approach, we identified dynamic expression patterns with distinct transcriptome signatures in oocytes and GCs, recognized the oocyte-GC communications during folliculogenesis and revealed putative biomarkers to predict ovarian reserve. In addition, we investigated the expression patterns of maternal-effect genes in human oocytes and propose their role in follicular development. Finally, we compared our data with the published oocyte transcriptome profiles from rodents and demonstrated robust interspecies differences.

RESULTS

Global Transcriptome Profiling of Human Oocytes and GCs

A total of 83 oocytes and 92 GC samples (each GC sample comprised randomly selected 10 cells per follicle owing to low abundancy of RNA in these cells) were obtained (Figure 1A). The data for MII oocytes were downloaded from our previous research[13] and merged with the newly generated data for the subsequent analyses. A down sampling analysis revealed adequate sequencing depth for gene expression detection (Figure S1D). After quality control and filtration of the RNA-Seq data, 80 oocytes and 71 GC samples were retained for the analysis (Figures S1). The unsupervised principal component analysis (PCA) showed there was a clear separation between 80 oocytes and 71 GCs with distinction between the developmental stages (Figure 1B). Next we analyzed the expression patterns of the known cell-type markers in the oocyte and GC clusters (Figure 1C and Figure 1D), which confirms the validity of PCA classification. Moreover, we selected the most variable genes that contributed to PC1 and could distinguish between the oocytes and GCs. In oocytes, the most variable genes included *NOL4*, *CTCTL*, *ITIH2*, *SNAP91* and *NAALAD2*. In GCs, the most variable genes were: *ZEB2*, *CD44*, *HSPG2*, *KDSR* and *SRRM3*The top oocyte or GCs-expressed variable genes ate presented in Figures 1E and 1F, respectively. the above observations suggest that the most variable genes between oocytes and GCs could be candidate cell type-specific markers.

Gene Expression Dynamics and Transcriptional Characteristics of Oocytes during Folliculogenesis

To explore the gene expression patterns in oocytes during folliculogenesis, we performed PCA analysis within the cohort of oocytes and observed five distinct subpopulations which corresponded morphological classification of follicular development (Figure 2A). The stage of follicular development was much more powerful discriminator than the sampling entity (Figure S1E), indicating that transcriptome profiles of oocytes reflect the physiological status of maturation, rather than genetic background. We then characterized the differentially expressed genes (DEGs) between the stages of follicle development in oocytes (FDR < 0.05; FC of $\log_2$ transformed FPKM > 1.5) (Figure 2B). A large number of these genes were under-expressed in primordial follicles with progressively increasing number of activated transcripts with follicular growth and maturation. The expression profiles of DEGs *RBM24*, *GPD1, NTF4* and *LCP2* were validated by using immunohistochemistry (IHC) on ovarian tissue from the scRNA-Seq sample set. Results showed that *RBM24* was expressed only in primordial and primary stage, *GPD1* was restricted secondary and antral stage, while *NTF4* and *LCP2* were specifically expressed in antral stage. These results are in agreement with the scRNA-Seq results (Figure 2E). To investigate possible biological functions of DEGs involved in folliculogenesis, we performed Gene Ontology (GO) analysis of DEGs in oocytes and revealed enriched biological processes in association with each stage of follicular development ($p < 0.05$) (Figure 2C).

We also investigated a number of germ cell markers and revealed some exhibited stable expression levels in oocytes during follicle development (e.g. *DDX4* and *ZP3*, Figure S2A), while others showed progressive upregulation with oocyte maturation (e.g. *ZP1, GDF9* and *H1FOO*). The expression of *ZP2*, *ZP3* and *ZP4* remained stable across all stages. Our findings suggest that *ZP1* might play a role in acquisition of oocyte competence and *ZP2*, *ZP3* and *ZP4* may act across all developmental stages in human oocytes. In contrast with our previous findings in fetal ovary [16,17], this study showed that the expression levels of pluripotency markers *NANOG* and *POU5F1* were constantly low during oocyte development, suggesting their different roles in fetal and adult ovary.

Next, we focused on investigating the expression patterns of meiosis-related genes in oocytes. The sets of 195 genes involved in meiosis I and 13 genes involved in meiosis II were gathered from the GO Consortium. Of these, 52 genes were differentially expressed across different stages of oocyte maturation. Most of the meiosis-specific genes demonstrated shift towards upregulation as maturation of oocytes proceeded, and exhibited strong over-expression in antral and preovulatory follicles (Figure 2D).

There is an ongoing lack of clarity regarding the levels of DNA methylation that determine change in DNA activity during human folliculogenesis. Here we demonstrated high expression levels of *DNMT1*, *DNMT3A* and *DNMT3B* in oocytes at all stages of folliculogenesis with mounting abundance (Figure S2A), which implies that DNA methylation level might be continually elevated with oocyte maturation. In

159 contrast to our previous study in PGCs [16], our results showed that ten-eleven
160 translocation (TET) family genes were under-expressed in oocytes at all stages of
161 development (Figure S2A). Together, overexpression of DNMT genes with loss of TET
162 activity indicates an active methylation transition in human oocyte during
163 folliculogenesis.

164 **Dynamic Expression and Transcriptional profiles of GCs during Folliculogenesis**

165 In GCs, PCA of all samples showed clustering into five groups according to stage of
166 follicular development (Figure 3A). An observed overlap between the clusters of
167 primary and secondary follicles indicated less pronounced difference at the
168 transcriptome level between these two stages. We then examined DEGs (FDR < 0.05;
169 FC of $\log_2$ transformed FPKM > 1.5) in GCs (Figure 3B). Interestingly, some of the
170 DEGs have been previously reported in association with oocyte competence, including
171 quality, maturity or fertilization rate, embryo quality and pregnancy outcomes [18,19] as
172 detailed in Table S2. GO analysis of DEGs (Figure 3C) revealed the crucial functional
173 roles of these genes during folliculogenesis. The expression profiles of the DEGs
174 *CDCA3*, *BNIPL* and *TST* were validated by using immunohistochemistry (IHC) on
175 ovarian tissue from the scRNA-Seq sample set (Figure 3E), which are in concordance
176 with the scRNA-Seq results.

177 Analysis of the cell-cycle genes involved in the G1/M and G2/S phases [20] in GCs
178 Revealed that at primordial stage, GCs were found to be relatively quiescent and
179 maintained low proliferative activity (Figure 3D). Both G1/S and G2/M-specific
180 genes were up-regulated in the GCs from primary, secondary and antral follicles. The

cell-cycle genes were predominantly abundantly expressed in the GCs from antral follicles, which designates their high proliferative activity at this stage. In contrast, the cell-cycle genes were down-regulated in the GCs from preovulatory follicles, which implies decreased degree of proliferation and differentiation in GCs at this stage.

Next, we focused on genes that have been previously associated with steroidogenesis (Figure S2B). *CYP11A1*, *CYP19A1*, *HSD3B1* and *HSD17B2*, encoding for steroidogenic enzymes, showed up-regulation in the antral follicles and reached peak expression levels in the preovulatory follicles. Their expression patterns indicate progressive increase in steroidogenic activity in maturing follicle, which culminates before ovulation. *NR5A1*, a key regulator of steroidogenic enzyme-encoding genes that has been previously described in sheep GCs [21], exhibited up-regulation with the progression of follicle growth. Both *ESR1* and *AR*, encoding for estradiol (E2) and androgen hormone receptors, respectively, were expressed in GCs at the primary follicle stage and reached highest expression level in antral follicles. This suggests E2 and androgens might control GC growth from the primordial follicle stage through these receptors.

Stage-Specific Signature Genes Identified in Oocytes and GCs

We identified a subset of stage-specific oocyte genes that were exclusively pertained to a single stage of folliculogenesis, which we referred to as “signature genes”. Conjointly, 382 signature genes were identified comprising the genes expressed in the oocytes from each stage (Figure S3A, Table S3). Distinct stage-specific expression patterns of *NTF4* and *LCP2* in oocytes were further confirmed by IHC staining (Figure 2E), which

showed that the expressions of these genes were restricted in antral stage. Of note, *NTF4*, proposed to facilitate follicle development in mouse by inducing FSH receptor (*FSHR*) [22], was exclusively expressed in oocytes from antral follicles (Figure 2E). We found that *FSHR* gene expression was pertained to GCs in antral follicles and was concordant to that of *NTF4* (Figure S3D). Our data suggested that *NTF4* might upregulates *FSHR* expression in human GCs and contributes to oocyte-to-GC crosstalk, thus plays an important role in oocyte development. For GCs, we also identified a subset of stage-specific signature genes during folliculogenesis (Figures S3C and S3D, Table S3). The expressions of signature genes *CDCA3* and *BNIPL* were validated by IHC (Figure 3E). Interestingly, *FSHR*, previously observed in somatic cells from early preantral to mature follicles in sheep [23], was exclusively expressed in the GCs from antral follicles in our study (Figure S3D), suggesting considerable inter-species differences. The full list of the signature genes in oocytes and GCs is presented in Table S3. These identified signature genes (Figure S3 and Table S3) could serve as candidate cell-specific markers for each follicle stage, allowing to establish the objective criteria for selecting competent oocytes in vitro.

Secretory Protein Coding Signature Genes

Certain specific oocyte- or neighboring GCs-derived genes could reflect the quantity and the quality of the follicles. Consequently, the peripherally secreted products of these genes may reveal prognostic information concerning ovarian reserve. Therefore, we searched for the secretory protein-coding signature genes that were exclusively pertained to either oocytes or GCs and were expressed either at early or at more

advanced stages of follicle development (as described in Methods). In total, we identified 51 protein-coding genes in oocytes and 17 in GCs that clustered into five groups (Figure S4). Cluster 1 comprised 16 oocyte genes with specific expression in the oocytes of primordial and primary follicles, suggesting they may reflect the primordial follicle pool. Cluster 2 included 19 oocyte genes with specific expression in the oocytes from secondary, antral and preovulatory follicles. Cluster 3 consisted of 27 oocyte genes that were represented across folliculogenesis. Cluster 4 (n = 4) and cluster 5 (n = 13) included GC-derived genes with specific expression at preovulatory and secondary-antral stages, respectively. The expression patterns of the genes from each cluster are exemplified in Figure S4B. These findings represent a potentially valuable source of candidate molecular biomarkers of ovarian reserve. Further evaluation of their expressions in biological fluids could contribute to development of ovarian reserve test.

Transcription Factors Regulatory Networks in Oocytes and GCs

To find the master regulators and construct the transcriptional regulatory network along the steps of human folliculogenesis, we utilized the ARACNe method to analyze all 1,469 known TFs from Animal Transcription Factor Database (TFDB v2.0) [24,25]. In the oocytes, the expressions of *GTF2I, CSDE1, SOHLH2, SMARCE1, TUB, HBP1, SOX30* and *HIF1A* were up-regulated in primary follicles, indicating that these TFs may play a critical role in the transition from primordial to primary stage (Figure 4). *KLF2, YBX2, FOXO6, SOX13, ETV5, TEAD2* and *OTX2* were over-expressed in the oocytes from secondary follicles compared to those from primary follicles, implying

they are likely the regulators of primary-to-secondary stage transition. *PINX1, PBX1, MTF1, SOX15, UBTF, SOX13,* and *POU2F1* had higher expressions in the oocytes from antral compared to secondary follicles, indicating their crucial regulatory roles in cytoplasmic and nuclear maturation of oocyte during antral stage. *ATF2* and *EOMES* were abundant in MII oocytes of preovulatory follicles, which indicates their potential role as TFs that possibly initiate the unique transcription networks involved in meiosis progression. Of note, we found that *SOX13* and *SOX15,* members of the SOX family of TFs, were up-regulated in the oocytes from secondary to antral follicles. While *SOX30* was found abundantly expressed in the oocytes during transition from primordial to primary follicle stages. This indicates their potential role in regulating transcription networks during primordial follicle activation (*SOX30*) and antral formation (*SOX13, SOX15*), respectively.

In the GCs, we found that *CREB1, NFKB1, MEF2A, PIAS1, FOSL2, KLF13* and *PRDM4* potentially regulated activation from the primordial to primary follicle stage, whereas *CRX, HES2, ZNF554, ZKSCAN3, LMX1B, FOXK1* and *SIX4* were the top candidate TFs possibly involved in transition from the primary to secondary follicle stage. *MBD1, FIZ1, GABPA, TGIF2, PIAS3, E4F1* and *IRF3* were likely driving initiation of the transcription network in antral follicles. *MEIS3, PRDM15* and *VTN* expressed in GCs of preovulatory follicles, could be the key regulators of cumulus cells progression in preovulatory follicles (Figure S5). Further evaluation of these TFs, their upstream signaling pathways, ligands, receptors and downstream targets in oocytes and GCs will provide insight into the transcriptional control of human folliculogenesis.

Key Signaling Pathways in Oocytes and GCs during Folliculogenesis

The Gene Set Enrichment Analysis (GSEA) and Kyoto Encyclopedia of Genes and Genomes (KEGG) analysis were applied to perform the pairwise comparisons of the follicular stages associated with each transition. There were 43 pathways overrepresented in the oocytes and 79 pathways enriched in the GCs from the primary follicles versus the primordial follicles ($p < 0.05$) (Table S4). Of these, the functional pathways that were significantly overrepresented both in oocytes and GCs ($p < 0.05$) and described in a context of folliculogenesis, included mTOR, GnRH, Neurotrophin and Insulin signaling (Figures S6A and S6B). These pathways probably mediate primordial-primary follicle transition and indicate the concerted action of the two follicular compartments. We identified 21 pathways enriched in the oocytes and 60 pathways in GCs that were overrepresented in antral, but not in secondary follicles ($p < 0.05$) (Table S4). In GCs, the steroid hormone biosynthesis was among the enriched pathways at the secondary-to-antral follicle transition, which indicates GCs play a key role in steroidogenesis at antral stage [26]. In addition, mTOR, Insulin and Neurotrophin pathways were over-represented in both primordial-to-primary and secondary-to-antral stages, suggesting a possibility for their involvement in these two transitions (Figures S6B, S6C and S6D). Interestingly, the enrichment of Neurotrophin pathway was concordant with the expression of its ligand *NTF4*, which was identified in this study as an antral stage-specific signature gene in oocyte (Figure 2E).

Bidirectional Interactions between the Oocyte and GC Compartments

To investigate interactions between oocyte and GCs, first we analyzed the expression of

291 the components of cell signaling pathways, including ligands, receptors and target
292 genes. NOTCH pathway was one of the significantly enriched in antral follicle GCs
293 （Table S4）. Expression of the components of NOTCH signaling revealed that ligands
294 *DLL3* and *JAG1* were predominantly expressed in early oocytes before preovulatory
295 stage. Their receptors *NOTCH2*, *NOTCH3* and the downstream target gene *HES1* were
296 highly expressed in GCs (Figure 5A). This finding highlights the role of NOTCH
297 signaling in oocyte-controlled proliferation and differentiation of GCs.
298 Then we analyzed the expression of the key components of TGF-β signaling pathway
299 in oocytes and GCs. Our data revealed that the expression levels of *GDF9* in oocytes
300 were high at all stages of follicular development, whereas *BMP15* was highly
301 expressed only in the oocytes from antral and preovulatory follicles (Figure 5B). This
302 observation points out that *GDF9* is likely to activate the TGF-β all through
303 folliculogenesis, while *BMP15* mostly exerts its role at more advanced stages. In
304 contrast, animal studies demonstrated that activation of the primordial follicles is
305 mediated by *BMP15* [27], suggesting it might play different roles in folliculogenesis
306 across the species.Interestingly, BMP type II receptor gene *BMPR2* and its target *ID3*
307 were expressed in both oocytes and GCs. The presence of gene and its target in two
308 different cell types, herein, allows to assume an existence of both autocrine and
309 paracrine mechanisms in BMP signaling.
310 In addition, we identified the components of GC-derived signaling involved in
311 folliculogenesis. For example, *KITLG* and its receptor *KIT,* previously implicated in
312 paracrine signaling in folliculogenesis, were expressed in GCs and oocytes,

313 respectively, which is consistent with previous findings in animal models [28]. *KITLG*
314 was expressed in primordial and upregulated in primary follicles with a subsequent
315 down-regulation, suggesting a possible role in primordial follicle activation (Figure S2).
316 Together, our findings provide evidence that human folliculogenesis is coordinated by
317 both autocrine and paracrine signaling pathway mechanisms that could be initiated by
318 either oocytes or GCs.

319 To understand the distribution of gap junctions in human follicles, we screened both
320 oocytes and GCs for the connexin (gap junction components) encoding genes,
321 previously reported in mammalian ovary, namely *GJB2* (Cx26), *GJB4* (Cx30.3), *GJB1*
322 (Cx32), *GJA4* (Cx37), *GJA5* (Cx40), *GJA1* (Cx43), *GJC1* (Cx45) and *GJA10* (Cx57) [29].
323 Three out of these genes exhibited compartment-specific pattern across the follicle
324 stages, while others were largely under-expressed. We identified that *GJC1* (Cx45) was
325 expressed only in the oocytes and *GJA1* (Cx43) was exclusively expressed in the GCs
326 at all follicle stages, while *GJA5* (Cx40) was pertained to the GCs of antral and
327 preovulatory follicles (Figure 5C). We speculate that the heterotypic (Cx43/Cx45 or
328 Cx40/Cx45) connexins might generate gap junction channels between oocyte and GCs,
329 while homotypic (Cx43 or Cx40) connexins may generate the channels between GCs.

330 **Global Expression Patterns of Maternal Effect Genes**

331 To explore the global expression profiles of maternal-effect genes, we integrated the
332 oocyte transcriptome data derived from this study with the transcriptome of human
333 preimplantation embryos that had been identified in our previous work [30]. We searched
334 for the genes that were expressed in MII oocytes and in zygotes, but not expressed in

8-cell embryos, as these genes are carried over from oocyte to early embryo and then get degraded following zygotic genome activation (ZGA). Overall, we identified 1,785 putative maternal genes. The unsupervised cluster analysis identified 4 clusters of genes according to expression patterns at specific stages of follicular growth (Figure S7A, Table S5). The genes in cluster 1 (n = 47) and cluster 2 (n = 588) were not expressed in primordial stage and upregulated during advanced stages of follicular maturation with peak expression in MII oocytes. However, the expression patterns in cluster 3 (n = 987) and cluster 4 (n = 163) showed that these transcripts could accumulate before primordial follicle assembly and potentially could be involved in early folliculogenesis and embryo development. The GO analysis revealed biological functions that have been reported in association with meiosis were among the overrepresented terms in cluster 2. While in cluster 3 and 4, genes were enriched in ubiquitous functions (Figure S7B).

Comparison of Human and Mouse Oocyte Transcriptomic Profiles during Folliculogenesis

Appraisal of the inter-species differences in oocyte transcriptome dynamics during all the stages of folliculogenesis is important to better understand the translational limitations of animal oocyte models, but such comparative data are largely lacking. Recent meta-analysis demonstrated substantial variation in oocyte transcriptome across different species [31]. To better understand the interspecies complexity of oocyte transcriptome in human and mice, and to provide a comparative view of gene expression in human and mice oocytes across folliculogenesis, we compared our

findings in human oocytes with reported RNA-Seq datasets produced from mice oocytes collected from primordial to antral stage. Mice RNA-Seq data were downloaded from Gahurova's study[32]. The standardized analytical approach to the merged raw data revealed a total of 23,091 genes expressed in human (our data) and 11,585 genes expressed in mice oocytes (Figure 6A).

We focused further analyses on 16,175 one-to-one homologous genes shared by human and mice, as per Mouse Genome Informatics (MGI) database [33], of which 14,431 genes were expressed in human oocytes and 9,964 genes were expressed in mice oocytes. There were 9,698 homologous genes that overlapped between human and mice oocyte samples. Of these, there were 6,115 house-keeping genes, 2,127 consistently expressed genes and 1,456 DEGs identified in this study as differentially expressed between different stages of folliculogenesis (Figures 6A). GO analysis of the co-expressed DEGs revealed that these genes exhibited ubiquitous functions, and none were specific for oocyte development (Figure 6B), which suggested that distinct molecular mechanisms may be involved during folliculogenesis in human and mouse. Moreover, several homologous DEGs implicated in oocyte development, such as *POU5F1,GJC1, TEAD2* and *BMP15*, showed different expression patterns in human and mice oocytes (Figure 6C).

Next, we assumed that oocyte genes with concordant expression pattern and high degree of correlation ($r > 0.8$) are involved in conserved molecular mechanisms in human and mice oocytes (Figure 6D). Notably, consistent homologous genes (*ZP3*, *RAC1*, *PATL2*), annotated in association with "oocyte maturation defect" in Online

379 Mendelian Inheritance in Man (OMIM) database, showed stable expression across
380 folliculogenesis in human and mice oocytes (Figure 6E), which proposes conserved
381 functional importance of these genes for oocyte development in both species. These
382 shared expression patterns suggested existence of evolutionary conserved mechanisms
383 involved in folliculogenesis and highlights the potentially significant translational
384 value of these conserved genes to the future research.

385 **Discussion**

386 This work describes the transcriptional landscape of the human oocytes and their
387 surrounding GCs across all major stages of folliculogenesis. To the best of our
388 knowledge, this is the first comprehensive investigation of human transcriptome from
389 both the germ cell and somatic follicle compartments in the adult ovary at single-cell
390 resolution. Previously, we have characterized the transcriptome profiles of human
391 pre-implantation embryos and PGCs with their gonadal niche at several stages of
392 development [16,17,30]. It is well established that oogenesis, folliculogenesis and
393 embryogenesis are sequential interrelated events, thus the transcriptome features of
394 both fetal oogenesis and adult folliculogenesis confer the underlying molecular
395 mechanisms of oocyte development. This body of work complements the findings from
396 our previous studies and contributes to a comprehensive overview of the transcriptional
397 events and their dynamics throughout the course of female gametogenesis with a
398 subsequent link to early pre-implantation embryo.

399 Previously, characterization of ovarian follicle in humans relied on evaluations of the

oocytes at certain stages of development or of the unseparated follicle compartments [12-14]. Although previous studies provided important insights into molecular events involved in folliculogenesis, generalizing the conclusions is made challenging by the multiple technical aspects related to different testing platforms and analytical variables. Tissue heterogeneity is one of the main predicaments of biological research when it is crucial to distinguish cell-specific profiles that reflect the in-vivo status. Laser Capture Microdissection (LCM) is increasingly used to harvest the cells of interest and to improve experimental precision, although faces challenges of compromised RNA quality and cell integrity [34]. To date, there have been no other studies that evaluated the transcriptomic profile across all the key stages of folliculogenesis and that performed parallel evaluations in both oocytes and GCs.

For the first time we demonstrated that each stage of folliculogenesis, defined by the morphological characteristics of both follicle compartments, had distinct transcriptome profile with different gene expression dynamics in oocytes and GCs. This finding supports the proposed, but not entirely proven concept that morphological classification of ovarian follicles reflects complex intrinsic transcriptional changes during folliculogenesis.

We also identified the candidate compartment-specific and stage-specific genes in both oocytes and GCs that provide a valuable clue for future more directed functional research. These findings may have important implication for development of essential genetic tools for cell-type-specific or stage-specific labeling and manipulations, which could be utilized in human follicle functional studies [35]. Further, an unmet need for the

422 reliable predictors of oocyte developmental competency drives discovery of new
423 biomarkers that would allow to establish more objective criteria for selecting
424 competent oocytes [36]. Previously reported biomarkers associated with successful
425 embryo development and pregnancy outcomes were mainly derived from GCs and
426 showed little consistency across the studies, which could be explained by the
427 differences in experimental methodology [18,19]. Some of the already proposed
428 biomarkers exhibited distinct expression patterns in our study, which makes them
429 particularly attractive candidates for further investigations. Of note, the functional
430 characteristics for majority of the gene markers identified in this study are
431 unrecognized and await further investigation.

432 In addition, we identified a subset of regulators of oocyte and GC transcriptome that
433 may be involved in follicle development and acquisition of oocyte competency. Further
434 evaluation of these TFs, their upstream signaling pathways, ligands, receptors and
435 downstream targets in oocytes and GCs will provide more understanding of the
436 transcriptional control of human folliculogenesis. These TFs may evolve as potential
437 targets for future therapeutic interventions to modulate follicle development.

438 It has been widely acknowledged that oocyte-granulosa bidirectional
439 communications are one of the core mechanisms involved in oocyte acquisition of
440 developmental competence [4]. Communication via signal transduction (e.g. signaling
441 pathways) and via direct cell-to-cell contact (e.g. gap junctions) provide molecular and
442 structural basis for effective oocyte-GC crosstalk required for follicular development.
443 However, precisely how oocyte-GC interact and how bi-directional communications

444 between the follicle compartments are initiated and maintained, is still unclear. In this
445 study we uncovered the signaling pathways that are coordinately and reciprocally
446 regulated in human oocytes and their surrounding GCs, by identifying the ligands and
447 their receptors that were derived from the reciprocal compartments, but shared the
448 expression pattern. This indicates that signaling pathways are activated by the ligands
449 derived from the germ cells that act on the neighboring gonadal somatic cells, and vice
450 versa. For example, in this study NOTCH signaling pathway, known important
451 regulator of cell-cell communication [37], was shown to be activated in GCs via
452 oocyte-driven mechanisms, which is in line with previously observed by our group in
453 fetal ovary [17]. In contrast, KITLG-KIT pathway was GC-driven, while TGF-β pathway
454 appeared to be activated through both autocrine and paracrine regulations. Single-cell
455 resolution made possible evaluation of the distinct gap junctional channels in human
456 follicles. We identified three different connexins, known to contribute to gap junctions
457 in animals, and we infer their involvement in gap junctions in humans, which so far has
458 been only demonstrated in animal models. Together, our findings provide further
459 insight into molecular basis of bidirectional interactions in both cell signaling pathway
460 and gap junction communications in human follicle. We support the notion that human
461 folliculogenesis is coordinated by both autocrine and paracrine signaling pathway
462 mechanisms that could be initiated by either oocytes or GCs.

463 In this study, we propose a set of candidate biomarkers that could be a valuable
464 source of information on reproductive potential and ovarian reserve. Ideally, an ovarian
465 reserve test should be easy to perform, reproducible and, importantly, should clearly

466 show evidence of improvements in patient reproductive outcomes following
467 test-directed interventions. However, none of the currently available ovarian reserve
468 tests, namely anti-Mullerian hormone (AMH) [38,39], follicle stimulating hormone (FSH)
469 and the antral follicle count (AFC) measured by transvaginal ultrasound [40,41] seem to
470 meet the above criteria. It is now understood that while ovarian reserve markers can
471 moderately predict response to stimulation in assisted reproductive technology (ART)
472 cycles, none of these tests determine the pregnancy potential and their role in general
473 population or in infertile women not undergoing ART treatment is not confirmed [10,42].
474 For instance, AMH, originating from the GCs of secondary and antral follicles, has
475 been initially accepted as the endocrine marker of FOR in humans [43]. However, it has
476 been recently proposed that AMH is not associated with the reproductive potential in
477 women of late reproductive age [8] and is a moderate predictor of menopause in general
478 population [9]. The main limitation of the current approach is inability to directly
479 measure ovarian reserve, since the biomarkers to determine the number or quality of
480 primordial follicles, a non-renewable pool that determines reproductive life span [44],
481 have yet to be identified. In addition, majority of the available biomarkers are secreted
482 by GCs and currently there is little information on oocyte-derived markers that provide
483 information on a status of follicle pool. Furthermore, it is possible to assume that
484 'all-purpose biomarker' does not exist, and different markers would be required to
485 address the specific outcome of interest. For example, reproductive potential in general
486 population is likely to be represented by the markers expressed at all stages of follicle
487 development, while age of menopause could be more accurately predicted by the

markers that originate in primordial pool. It is also possible that response to fertility treatments and pregnancy outcomes may be better predicted by the markers confined to the antral follicles, the main targets of ovarian stimulation gonadotropin treatments, while the predictors of natural pregnancy outcomes may be secreted by the more advanced follicles. Until new data emerge, these questions will remain open. Further research to elucidate the biological roles of the proposed candidates, in conjunction with comprehensive evaluation of their expression levels in biological fluids could contribute to advancements in development of clinically informative ovarian reserve test.

In this study we offer further insights on species-specific gene expression during folliculogenesis. Mouse models are a mainstay of translational biomedical research and are widely implicated in the investigations of ovarian transcriptome. Mice are poly-ovulating species, breed readily, inexpensive and easy to handle, which makes them ideal candidates for laboratory experiments. Besides, mice and humans are at least 95% genetically identical, which allows to assume conservation of fundamental biological processes across the species. However, it has been previously reported that the oocyte transcriptome is highly variable across mammals and the human oocyte is likely to have a greater complexity than other mammals [31,45]. Appraisal of the inter-species differences in oocyte transcriptome dynamics during all the stages of folliculogenesis is important to better understand the translational limitations of animal oocyte models, but such comparative data are largely lacking. We evidenced strong transcriptional activity in both human and mouse oocytes, which dominated in humans

and demonstrated considerable variability in oocyte transcriptome between human and mouse. We revealed different gene expression dynamics during folliculogenesis in both species and thus, propose a cautious approach when mice oocyte data are applied to the human domain. We also showed some degree of similarity in gene expression between human and mice oocytes, which highlights the potentially significant translational value of these conserved genes to the future research. We do not suggest that the mouse is an invalid experimental system for studying human oocytes. Rather, we provide a database for further investigations of the molecular mechanisms associated with oocyte development through mouse models, and improve the understanding on how well the oocyte transcriptome data translate from mouse to human.

It is important to mention that our study is not devoid of limitations. Firstly, despite rigorous experimental approach and robust analyses, our findings are not sufficient to confirm the functional characteristics of the identified transcripts. Rather, our data offer a comprehensive resource for future more directed functional studies in oocyte research. Next, our methods relied on the mechanical or enzymatic dissociation of follicular compartments, thus the information on temporal and spatial regulation of gene expression in GCs was not reflected. The recently proposed Geo-Seq protocol allows the profiling of transcriptome information from only a small number cells and retains their native spatial information [34], which will help in future investigations of gene expression with positional information. Finally, low number of MII oocytes included in this study could undermine the reliability of the results for this group, although satisfactory gene number and considerable homogeneity of the expression

data from these cells suggest adequate quality of the data.

In summary, understanding molecular events involved in folliculogenesis remains a key challenge for reproductive biology research with limited availability of human follicles for research being the main constrain. By using a high-resolution transcriptome analysis for single oocyte and its surrounding GCs, we recapitulated a cascade of the molecular events involved in folliculogenesis. This work contributes to the collaborative effort to strengthen our understanding of reproductive function, which may assist with the development of more targeted future interventions to improve oocyte competence in-vitro and in-vivo.

METHODS

Collection of Human Ovarian Tissue Samples

With oral and written informed consent, fresh ovarian tissues were taken from 7 female donors who underwent ovariectomy for the following indications: sex reassignment surgery (n = 1), fertility preservation for cervical cancer (n = 1), endometrial cancer (n = 2), benign ovarian mass (n = 2) and lymphoma (n = 1). All the donors were of reproductive age, ranging 24 to 32 years (median age of 28 years). All the participants had regular menstrual cycles, had no history of autoimmune or genetic conditions. None of the tissue donors were on hormonal treatment at least 6 months before surgery, had no previous ovarian surgery and were not exposed to any cytotoxic agents or radiotherapy. All the samples had normal histopathology (described below). The ovarian tissue samples were collected in operation theatre during the procedure, immediately transferred to the laboratory and treated as previously described [46]. Briefly, the human ovarian tissues were collected in the operation theatre and transported to the laboratory in Leibovitz's L-15 medium (Sigma-Aldrich) on ice with the supplementation of 1% human serum albumin (Life Technologies, Carlsbad, CA), 100 IU/mL streptomycin (Sigma, St. Louis, MO) and 100 µg/mL penicillin (Sigma, St. Louis, MO). Scalpel and surgical scissors were used to enucleate the medulla tissues. Then scalpel was used to cut the ovarian cortical tissues into small ovarian pieces with a size of 5 mm×5 mm×1 mm.

Ovarian Histology Assessment

Histological assessment was performed on all the ovarian tissue samples by using

564 hematoxylin and eosin (HE) staining as described elsewhere [47]. After fixation, the
565 samples were paraffin embedded and cut into serial sections of 5-μm-thick. All the
566 prepared tissue sections were reviewed by two independent pathologists and confirmed
567 normal ovarian tissues.

568 **Immunohistochemistry**

569 Immunohistochemistry staining of the ovarian tissue samples that were utilized in
570 this study for RNA-Seq experiments was performed by using the ABC Staining
571 System (Zhongshan Golden Bridge Biotechnology, Inc., Beijing, China), as
572 previously described [48]. Brown staining of the cytoplasm or nucleus of the cells was
573 considered as positive.

574 **Isolation of Human Oocytes and GCs**

575 Human follicles were isolated from fresh ovarian tissues as described previously [49,50].
576 Briefly, after removal of medulla tissues, the ovarian cortical pieces were placed in a
577 tissue sectioner (McIlwain Tissue Chopper, The Mickle Laboratory, Guildford, UK)
578 and cut into 0.5 × 0.5 × 1 mm pieces. Then the tissue pieces were enzymatically
579 digested by a mixed digestion medium, which included αMEM (Sigma-Aldrich)
580 media, 0.04 mg/ml Liberase DH (Dispase High; Roche Diagnostics GmbH,
581 Mannheim, Germany), 10 IU/ml DNase I (Sigma-Aldrich), 100 IU/ml penicillin and
582 100 μg/ml streptomycin (Invitrogen) and incubated for 75 min on a shaker at 37°C
583 (Thermo Fisher, Marietta, OH, USA). The incubation was terminated by double wash
584 with DPBS (Sigma-Aldrich) supplemented with 10% HSA (LifeGlobal). Then the
585 follicles were isolated mechanically using 29G needles and were transferred to culture

586 medium. Subsequently, the single oocytes and GCs were enzymatically separated with
587 accutase (Sigma-Aldrich) and were mechanically isolated by using 29G needles. GC
588 samples comprised randomly selected 10 cells per sample because of low abundancy of
589 RNA in these cells. GCs from the antral and preovulatory follicles included cumulus
590 cells isolated from the cumulus-oocyte complex (COC) as following: 6 samples of
591 cumulus cells from the antral follicles and 16 samples from the preovulatory follicles.
592 Follicle stages were classified according to the criteria described by Gougeon [51]. The
593 diameters of follicles and oocytes were measured under light microscope (Nikon).

594 **Single-Cell cDNA Libraries Construction from Oocytes and GCs**

595 The oocytes and GCs that were isolated from follicles were analyzed by scRNA-Seq as
596 previously described [30,52]. Briefly, the single oocytes or 10 randomly selected GCs were
597 transferred into the lysis buffer quickly using a mouth pipette. Then we performed
598 reverse transcription on the cell lysate and terminal deoxynucleotidyl transferase was
599 adopted to add a poly A tail to the 3′ end of the first-strand cDNAs, next we performed
600 20 cycles of PCR to amplify the single-cell cDNA library. qPCR analysis was
601 conducted to check the quality of the cDNA libraries using housekeeping genes
602 (GAPDH and RPS24). The RNA-Seq libraries were constructed by a Kappa Hyper
603 Prep Kit (Kappa Biosystems).

604 **RNA-Seq Data Processing**

605 The analysis of single-cell RNA-Seq data was carried out as previously described
606 [16,17,53]. Briefly, RNA-Seq raw reads with 10% low quality bases, adapters and artificial
607 sequences (including UP1, UP2, polyA sequences) introduced during the experimental

608 processes were trimmed by in house scripts. Next, the trimmed clean reads were
609 aligned to the UCSC human hg19 reference using Tophat2 (v2.1.0) with default
610 settings [54]. Cufflinks (v2.2.1) was further used to quantify transcription levels of
611 annotated genes [55].

612 Previous published data, including those from human MII oocytes [30], human
613 pre-implantation embryos [30], and mouse oocytes [56,57], were downloaded from the GEO
614 data sets, and the raw fastq reads were obtained and incorporated into our analysis. For
615 all sequenced cells, we counted the number of genes detected in each cell. Cells with
616 fewer than 2,400 genes or 500,000 mapped reads were filtered out. In total, 80 oocytes
617 and 71 GCs at five developmental stages passed the filter standards. To ensure the
618 accuracy of estimated gene expression levels, only genes with FPKM > 1 in at least
619 one cell were analyzed[58]. Expression levels of each gene were plus one then log2
620 transformed in the following analysis. Expression levels of each oocyte and GC were
621 in Table S1.

622 **Principal Component Analysis (PCA)**

623 The Seurat method was applied to analyze the single-cell data (77 unmatured oocytes,
624 three matured MII oocytes and 71 GCs) to observe the whole clustering profile [59]. Only
625 highly variable genes (coefficient of variation $>$ 0.5) were used as inputs for PCA. And
626 the marker genes in PCA plot were plotted by the FeaturePlot function in Seurat
627 package. To complement the PCA clustering more accurately, we also clustered the
628 oocytes and GCs separately using the FactoMineR package in R [60].

629 **Identification of DEGs and Gene Ontology Analysis**

630 Multiple t-test was used to obtain the statistical significance of differentially expressed
631 genes in each stage. Only the genes with significant p-values and false discovery rate
632 (FDR) less than 0.05 with a fold change of log2 transformed FPKM larger than 1.5
633 were considered to be differentially expressed. Gene ontology analysis of differentially
634 expressed genes was performed using DAVID [61].

635 **Identifying Expression Patterns of Maternal Effect Gene**

636 Maternal effect genes play a critical role before zygote genome activation (ZGA). It's
637 reported that ZGA mainly happened at 4 cells to 8 cells stages [30,62].To explore the
638 expression patterns of maternal effect genes during folliculogenesis，we searched for
639 genes carried from oocytes to early embryo and degraded before ZGA. Genes
640 expressed (FPKM > 1) at MII and zygote stage but relatively low expressed (FPKM <
641 1) at 8 cells stage were taken as candidates. The candidate genes were clustered by
642 expression correlation and cut into four clusters with cutree function in R.

643 **Identifying Secretory Protein Coding Signature Genes**

644 To identify candidate biomarkers for predicting ovarian reserve, we focused on the
645 oocyte- or GC-derived secretory proteins. The secretory protein encoding genes were
646 downloaded from the Human Protein Atlas database (https://www.proteinatlas.org/).
647 The GTEx v6 database (https://www.gtexportal.org) was utilized to obtain
648 information on gene expression level in tissues of interest. We aimed to evaluate only
649 protein secreting genes expressed in ovary and therefore we focused on genes that
650 were previously identified only in gonads and could be present in brain, but not in any

651 other tissues [63]. We assumed that brain-blood (B-B) barrier prevents secretion of the
652 proteins into systemic circulation and thus reduces confounding effect on peripheral
653 levels of these proteins. This assumption was based on the previously observed high
654 levels of AMH in brain, which supports the idea of restrictive function of B-B barrier
655 [64].

656 **Transcription Factor Network Construction**

657 Transcription factors play a key role in regulating development. To find the driver
658 factors and construct their regulatory network in each two consecutive stages, we used
659 ARACNe to perform the regulatory network analysis as described previously [17]. First,
660 the 1,469 human transcription factors in AnimalTFDB [25] and gene expression matrix
661 were taken as inputs for ARACNe-AP software [25]. Then, viper package in R was used
662 to visualize the transcription factors and their target genes in each consecutive stage [65].
663 Regulators with p-values less than 0.01 were inferred as driver factors in each two
664 consecutive stages.

665 **GSEA Analysis**

666 To identify the significant enriched pathways in each two consecutive development
667 stages, we used Gene Set Enrichment Analysis (GSEA,
668 http://software.broadinstitute.org/gsea/index.jsp) to perform enrichment analysis, and
669 the KEGG pathway was used [66]. The gene sets that showed nominal p-value less than
670 0.05 were chosen as enriched.

671 **Analysis of Conservation Between Human and Mouse**

672 Human and mouse homologous genes were downloaded from Vertebrate Homology

673 Database (http://www.informatics.jax.org/homology.shtml). Housekeeping genes
674 were obtained from Human Protein Atlas. Human oocytes expressed genes were
675 overlapped with mouse oocytes expressed homologous genes to find genes expressed
676 in both human and mouse oocytes, and the housekeeping genes were filtered out from
677 the overlapped gene set. The retained genes were divided as homologous DEGs
678 (genes in DEGs of human oocytes) and homologous non-DEGs. The genes involved
679 in oocyte maturation defect were downloaded from Online Mendelian Inheritance in
680 Man (OMIM) database (https://www.omim.org/) and incorporated in to analysis.
681

682 **References:**

683 1 Eppig, J. J., Wigglesworth, K. & Pendola, F. L. The mammalian oocyte orchestrates the rate of
684 ovarian follicular development. *Proceedings of the National Academy of Sciences of the*
685 *United States of America* **99**, 2890-2894, doi:10.1073/pnas.052658699 (2002).
686 2 Moley, K. H. & Schreiber, J. R. Ovarian follicular growth, ovulation and atresia. Endocrine,
687 paracrine and autocrine regulation. *Advances in experimental medicine and biology* **377**,
688 103-119 (1995).
689 3 Sanchez, F. & Smitz, J. Molecular control of oogenesis. *Biochimica et biophysica acta* **1822**,
690 1896-1912, doi:10.1016/j.bbadis.2012.05.013 (2012).
691 4 Li, R. & Albertini, D. F. The road to maturation: somatic cell interaction and self-organization
692 of the mammalian oocyte. *Nature reviews. Molecular cell biology* **14**, 141-152,
693 doi:10.1038/nrm3531 (2013).
694 5 Zhang, K. & Smith, G. W. Maternal control of early embryogenesis in mammals.
695 *Reproduction, fertility, and development* **27**, 880-896, doi:10.1071/RD14441 (2015).
696 6 Jukam, D., Shariati, S. A. M. & Skotheim, J. M. Zygotic Genome Activation in Vertebrates.
697 *Developmental cell* **42**, 316-332, doi:10.1016/j.devcel.2017.07.026 (2017).
698 7 Gleicher, N., Weghofer, A. & Barad, D. H. Defining ovarian reserve to better understand
699 ovarian aging. *Reproductive biology and endocrinology : RB&E* **9**, 23,
700 doi:10.1186/1477-7827-9-23 (2011).
701 8 Steiner, A. Z. *et al.* Association Between Biomarkers of Ovarian Reserve and Infertility
702 Among Older Women of Reproductive Age. *Jama* **318**, 1367-1376,
703 doi:10.1001/jama.2017.14588 (2017).
704 9 Depmann, M. *et al.* Does anti-Mullerian hormone predict menopause in the general
705 population? Results of a prospective ongoing cohort study. *Human reproduction* **31**,
706 1579-1587, doi:10.1093/humrep/dew112 (2016).
707 10 Jirge, P. R. Ovarian reserve tests. *Journal of human reproductive sciences* **4**, 108-113,
708 doi:10.4103/0974-1208.92283 (2011).
709 11 Knight, P. G. & Glister, C. TGF-beta superfamily members and ovarian follicle development.
710 *Reproduction* **132**, 191-206, doi:10.1530/rep.1.01074 (2006).
711 12 Grondahl, M. L. *et al.* The dormant and the fully competent oocyte: comparing the
712 transcriptome of human oocytes from primordial follicles and in metaphase II. *Molecular*
713 *human reproduction* **19**, 600-617, doi:10.1093/molehr/gat027 (2013).

13 Kristensen, S. G., Ebbesen, P. & Andersen, C. Y. Transcriptional profiling of five isolated size-matched stages of human preantral follicles. *Molecular and cellular endocrinology* **401**, 189-201, doi:10.1016/j.mce.2014.12.012 (2015).

14 Markholt, S. *et al.* Global gene analysis of oocytes from early stages in human folliculogenesis shows high expression of novel genes in reproduction. *Molecular human reproduction* **18**, 96-110, doi:10.1093/molehr/gar083 (2012).

15 Picelli, S. Single-cell RNA-sequencing: The future of genome biology is now. *RNA biology* **14**, 637-650, doi:10.1080/15476286.2016.1201618 (2017).

16 Guo, F. *et al.* The Transcriptome and DNA Methylome Landscapes of Human Primordial Germ Cells. *Cell* **161**, 1437-1452, doi:10.1016/j.cell.2015.05.015 (2015).

17 Li, L. *et al.* Single-Cell RNA-Seq Analysis Maps Development of Human Germline Cells and Gonadal Niche Interactions. *Cell stem cell* **20**, 858-873 e854, doi:10.1016/j.stem.2017.03.007 (2017).

18 Huang, Z. & Wells, D. The human oocyte and cumulus cells relationship: new insights from the cumulus cell transcriptome. *Molecular human reproduction* **16**, 715-725, doi:10.1093/molehr/gaq031 (2010).

19 Parks, J. C. *et al.* Corona cell RNA sequencing from individual oocytes revealed transcripts and pathways linked to euploid oocyte competence and live birth. *Reproductive biomedicine online* **32**, 518-526, doi:10.1016/j.rbmo.2016.02.002 (2016).

20 Tirosh, I. *et al.* Dissecting the multicellular ecosystem of metastatic melanoma by single-cell RNA-seq. *Science* **352**, 189-196, doi:10.1126/science.aad0501 (2016).

21 Bonnet, A. *et al.* An overview of gene expression dynamics during early ovarian folliculogenesis: specificity of follicular compartments and bi-directional dialog. *BMC genomics* **14**, 904, doi:10.1186/1471-2164-14-904 (2013).

22 Kerr, B., Garcia-Rudaz, C., Dorfman, M., Paredes, A. & Ojeda, S. R. NTRK1 and NTRK2 receptors facilitate follicle assembly and early follicular development in the mouse ovary. *Reproduction* **138**, 131-140, doi:10.1530/REP-08-0474 (2009).

23 Tisdall, D. J., Watanabe, K., Hudson, N. L., Smith, P. & McNatty, K. P. FSH receptor gene expression during ovarian follicle development in sheep. *Journal of molecular endocrinology* **15**, 273-281 (1995).

24 Margolin, A. A. *et al.* ARACNE: an algorithm for the reconstruction of gene regulatory networks in a mammalian cellular context. *BMC bioinformatics* **7 Suppl 1**, S7, doi:10.1186/1471-2105-7-S1-S7 (2006).

25 Zhang, H. M. *et al.* AnimalTFDB: a comprehensive animal transcription factor database. *Nucleic acids research* **40**, D144-149, doi:10.1093/nar/gkr965 (2012).

26 Mingoti, G. Z., Garcia, J. M. & Rosa-e-Silva, A. A. Steroidogenesis in cumulus cells of bovine cumulus-oocyte-complexes matured in vitro with BSA and different concentrations of steroids. *Animal reproduction science* **69**, 175-186 (2002).

27 Kim, J. Y. Control of ovarian primordial follicle activation. *Clinical and experimental reproductive medicine* **39**, 10-14, doi:10.5653/cerm.2012.39.1.10 (2012).

28 Thomas, F. H. & Vanderhyden, B. C. Oocyte-granulosa cell interactions during mouse follicular development: regulation of kit ligand expression and its role in oocyte growth. *Reproductive biology and endocrinology : RB&E* **4**, 19, doi:10.1186/1477-7827-4-19 (2006).

29 Gershon, E., Plaks, V. & Dekel, N. Gap junctions in the ovary: expression, localization and function. *Molecular and cellular endocrinology* **282**, 18-25, doi:10.1016/j.mce.2007.11.001 (2008).

30 Yan, L. *et al.* Single-cell RNA-Seq profiling of human preimplantation embryos and embryonic stem cells. *Nature structural & molecular biology* **20**, 1131-1139, doi:10.1038/nsmb.2660 (2013).

31 Biase, F. H. Oocyte Developmental Competence: Insights from Cross-Species Differential Gene Expression and Human Oocyte-Specific Functional Gene Networks. *Omics : a journal of integrative biology* **21**, 156-168, doi:10.1089/omi.2016.0177 (2017).

32 Gahurova, L. *et al.* Transcription and chromatin determinants of de novo DNA methylation timing in oocytes. *Epigenetics Chromatin* **10**, 25, doi:10.1186/s13072-017-0133-5 (2017).

33 Blake, J. A. *et al.* Mouse Genome Database (MGD)-2017: community knowledge resource for the laboratory mouse. *Nucleic acids research* **45**, D723-D729, doi:10.1093/nar/gkw1040 (2017).

34 Chen, J. *et al.* Spatial transcriptomic analysis of cryosectioned tissue samples with Geo-seq. *Nature protocols* **12**, 566-580, doi:10.1038/nprot.2017.003 (2017).

35 Zuccotti, M., Merico, V., Cecconi, S., Redi, C. A. & Garagna, S. What does it take to make a developmentally competent mammalian egg? *Human reproduction update* **17**, 525-540, doi:10.1093/humupd/dmr009 (2011).

36 Patrizio, P., Fragouli, E., Bianchi, V., Borini, A. & Wells, D. Molecular methods for selection of the ideal oocyte. *Reproductive biomedicine online* **15**, 346-353 (2007).

37 Vanorny, D. A. & Mayo, K. E. The role of Notch signaling in the mammalian ovary. *Reproduction* **153**, R187-R204, doi:10.1530/REP-16-0689 (2017).

780 38 Freeman, E. W., Sammel, M. D., Lin, H. & Gracia, C. R. Anti-mullerian hormone as a
781 predictor of time to menopause in late reproductive age women. *The Journal of clinical*
782 *endocrinology and metabolism* **97**, 1673-1680, doi:10.1210/jc.2011-3032 (2012).
783 39 Dolleman, M. *et al.* Anti-Mullerian hormone is a more accurate predictor of individual time to
784 menopause than mother's age at menopause. *Human reproduction* **29**, 584-591,
785 doi:10.1093/humrep/det446 (2014).
786 40 Hendriks, D. J. *et al.* Repeated clomiphene citrate challenge testing in the prediction of
787 outcome in IVF: a comparison with basal markers for ovarian reserve. *Human reproduction*
788 **20**, 163-169, doi:10.1093/humrep/deh553 (2005).
789 41 Wellons, M. F. *et al.* Antral follicle count predicts natural menopause in a population-based
790 sample: the Coronary Artery Risk Development in Young Adults Women's Study. *Menopause*
791 **20**, 825-830, doi:10.1097/GME.0b013e31827f06c2 (2013).
792 42 Gleicher, N., Weghofer, A. & Barad, D. H. The role of androgens in follicle maturation and
793 ovulation induction: friend or foe of infertility treatment? *Reproductive biology and*
794 *endocrinology : RB&E* **9**, 116, doi:10.1186/1477-7827-9-116 (2011).
795 43 Peluso, C. *et al.* AMH: An ovarian reserve biomarker in assisted reproduction. *Clinica*
796 *chimica acta; international journal of clinical chemistry* **437**, 175-182,
797 doi:10.1016/j.cca.2014.07.029 (2014).
798 44 Wallace, W. H. & Kelsey, T. W. Human ovarian reserve from conception to the menopause.
799 *PloS one* **5**, e8772, doi:10.1371/journal.pone.0008772 (2010).
800 45 Sylvestre, E. L. *et al.* Evolutionary conservation of the oocyte transcriptome among
801 vertebrates and its implications for understanding human reproductive function. *Molecular*
802 *human reproduction* **19**, 369-379, doi:10.1093/molehr/gat006 (2013).
803 46 Zhang, Y. *et al.* Mesenchymal stem cell-derived angiogenin promotes primodial follicle
804 survival and angiogenesis in transplanted human ovarian tissue. *Reproductive biology and*
805 *endocrinology : RB&E* **15**, 18, doi:10.1186/s12958-017-0235-8 (2017).
806 47 Xia, X. *et al.* Mesenchymal Stem Cells Enhance Angiogenesis and Follicle Survival in Human
807 Cryopreserved Ovarian Cortex Transplantation. *Cell transplantation* **24**, 1999-2010,
808 doi:10.3727/096368914X685267 (2015).
809 48 Gao, J. M. *et al.* Improvement in the quality of heterotopic allotransplanted mouse ovarian
810 tissues with basic fibroblast growth factor and fibrin hydrogel. *Human reproduction* **28**,
811 2784-2793, doi:10.1093/humrep/det296 (2013).
812 49 Wang, T. R. *et al.* Basic fibroblast growth factor promotes the development of human ovarian

813 early follicles during growth in vitro. *Human reproduction* **29**, 568-576,
814 doi:10.1093/humrep/det465 (2014).
815 50 Vanacker, J. *et al.* Enzymatic isolation of human primordial and primary ovarian follicles with
816 Liberase DH: protocol for application in a clinical setting. *Fertility and sterility* **96**, 379-383
817 e373, doi:10.1016/j.fertnstert.2011.05.075 (2011).
818 51 Gougeon, A. Dynamics of follicular growth in the human: a model from preliminary results.
819 *Human reproduction* **1**, 81-87 (1986).
820 52 Wang, T. R. *et al.* Human single follicle growth in vitro from cryopreserved ovarian tissue
821 after slow freezing or vitrification. *Human reproduction* **31**, 763-773,
822 doi:10.1093/humrep/dew005 (2016).
823 53 Zhou, F. *et al.* Tracing haematopoietic stem cell formation at single-cell resolution. *Nature*
824 **533**, 487-492, doi:10.1038/nature17997 (2016).
825 54 Trapnell, C., Pachter, L. & Salzberg, S. L. TopHat: discovering splice junctions with RNA-Seq.
826 *Bioinformatics* **25**, 1105-1111, doi:10.1093/bioinformatics/btp120 (2009).
827 55 Trapnell, C. *et al.* Transcript assembly and quantification by RNA-Seq reveals unannotated
828 transcripts and isoform switching during cell differentiation. *Nature biotechnology* **28**,
829 511-515, doi:10.1038/nbt.1621 (2010).
830 56 Veselovska, L. *et al.* Deep sequencing and de novo assembly of the mouse oocyte
831 transcriptome define the contribution of transcription to the DNA methylation landscape.
832 *Genome biology* **16**, 209, doi:10.1186/s13059-015-0769-z (2015).
833 57 Hikabe, O. *et al.* Reconstitution in vitro of the entire cycle of the mouse female germ line.
834 *Nature* **539**, 299-303, doi:10.1038/nature20104 (2016).
835 58 Treutlein, B. *et al.* Reconstructing lineage hierarchies of the distal lung epithelium using
836 single-cell RNA-seq. *Nature* **509**, 371-375, doi:10.1038/nature13173 (2014).
837 59 Macosko, E. Z. *et al.* Highly Parallel Genome-wide Expression Profiling of Individual Cells
838 Using Nanoliter Droplets. *Cell* **161**, 1202-1214, doi:10.1016/j.cell.2015.05.002 (2015).
839 60 Metsalu, T. & Vilo, J. ClustVis: a web tool for visualizing clustering of multivariate data using
840 Principal Component Analysis and heatmap. *Nucleic acids research* **43**, W566-570,
841 doi:10.1093/nar/gkv468 (2015).
842 61 Huang da, W., Sherman, B. T. & Lempicki, R. A. Systematic and integrative analysis of large
843 gene lists using DAVID bioinformatics resources. *Nature protocols* **4**, 44-57,
844 doi:10.1038/nprot.2008.211 (2009).
845 62 Braude, P., Bolton, V. & Moore, S. Human gene expression first occurs between the four- and

eight-cell stages of preimplantation development. *Nature* **332**, 459-461, doi:10.1038/332459a0 (1988).

63 Uhlen, M. *et al.* Proteomics. Tissue-based map of the human proteome. *Science* **347**, 1260419, doi:10.1126/science.1260419 (2015).

64 Haddad-Tovolli, R., Dragano, N. R. V., Ramalho, A. F. S. & Velloso, L. A. Development and Function of the Blood-Brain Barrier in the Context of Metabolic Control. *Frontiers in neuroscience* **11**, 224, doi:10.3389/fnins.2017.00224 (2017).

65 Alvarez, M. J. *et al.* Functional characterization of somatic mutations in cancer using network-based inference of protein activity. *Nature genetics* **48**, 838-847, doi:10.1038/ng.3593 (2016).

66 Subramanian, A. *et al.* Gene set enrichment analysis: a knowledge-based approach for interpreting genome-wide expression profiles. *Proceedings of the National Academy of Sciences of the United States of America* **102**, 15545-15550, doi:10.1073/pnas.0506580102 (2005).

Figure legends

Figure 1. The Global Transcriptome Patterns of Human Oocytes and granulosa cells（GCs).

A) Schematic illustration of the study workflow.

Primordial - primordial follicles; Primary - primary follicles; Secondary - secondary follicles; Antral - antral follicles; Preovulatory - preovulatory follicles; GCs - granulosa cells.

B) Principal component analysis (PCA) of the transcriptome of scRNA-Seq data from all oocytes and GCs included in this study. The PC1 separates two follicular compartments (oocytes vs. GCs). The PC2 separates the samples according to their follicular stages. Red color indicates oocytes, blue color indicates GCs. The sizes of the points represent follicles of different sizes.

C) Expression patterns of oocyte marker genes exhibited on PCA plots; a gradient of gray to red indicates the low to high gene expression level.

D) Expression patterns of GC marker genes exhibited on PCA plots.

E) Expression of the candidate cell-type specific markers of oocytes on PCA plots.

F) Expression of the candidate cell-type specific markers of GCs on PCA plots.

Figure 2. Gene Expression Dynamics and Transcriptional Characteristics of Oocytes.

A) Principal component analysis (PCA) of the transcriptome of scRNA-Seq data from 80 oocytes collected from follicles at different stages of development. Oocytes are clustered into five subpopulations corresponding to morphological stages.

884 Different colors and sizes of the points represent follicles of different stages and sizes,
885 respectively. See also Figure S1E for the results of PCA that portrays sampling
886 entities within the oocytes.
887 B) Heatmap of all the differentially expressed genes (DEGs) in oocytes at five stages
888 of folliculogenesis. The numbers of identified DEGs are indicated on the y-axis, and
889 the stages of follicle development are presented along the x-axis. The color key from
890 blue to red indicates the relative gene expression level from low to high, respectively.
891 C) Significantly enriched GO terms (biological processes) of DEGs in oocytes at five
892 stages of folliculogenesis.
893 D) Heatmap of genes involved in meiosis that are differentially expressed in oocytes
894 at five stages of folliculogenesis.
895 E) Immunohistochemistry staining of selected DEGs. The boxplot demonstrating
896 gene expression level is presented on the left of each corresponding
897 immunohistochemistry panel. White triangles indicate the follicles. Scale bar, 100
898 μm.
899 **Figure 3. Dynamic Gene Expression Patterns and Transcriptional Features in**
900 **GCs.**
901 A) Principal component analysis (PCA) of the transcriptome of scRNA-Seq data
902 from 71 GCs collected from follicles at different stages of development. GCs are
903 clustered into five subpopulations. Different colors and sizes of the points represent
904 follicles of different stages and sizes, respectively.
905 B) Heatmap of all the differentially expressed genes (DEGs) in GCs at five stages of

folliculogenesis. The numbers of identified DEGs are indicated on the y-axis, and the stages of follicle development are presented along the x-axis. The color key from blue to red indicates the relative gene expression level from low to high, respectively.

C) Significantly enriched GO terms (biological processes) of DEGs in GCs at five stages of folliculogenesis.

D) Heatmap of cell-cycle related genes that are expressed in GCs at five stages of folliculogenesis.

E) Immunohistochemistry staining of selected DEGs. The boxplot demonstrating gene expression level is presented on the left of each corresponding immunohistochemistry panel. White triangles indicate the follicles. Scale bar, 100 μm.

Figure 4. Inferred Key Transcriptional Factors in Oocytes at Each Stage-to-stage Transition of Folliculogenesis.

A) MARINa plots of targets for each candidate master regulator. Red vertical bar represents the activated targets, blue represents the repressed targets. On the x axis, genes are rank-sorted according to the significance of differential expression between the two developmental stages. The candidate master regulators are displayed on the right. The corresponding p-values of these master regulators indicate the significance of enrichment are displayed on the left. See also Figure S4 for the analogous information in GCs.

B) Violin plots show the relative expression levels (log2 [FPKM+1]) of each master regulator in two consecutive stages. See also Figure S4 for the analogous information in

928 GCs.

929 **Figure 5. Signaling Pathways and Gap Junction Involved in Oocyte-GC**
930 **Crosstalk.**

931 A) NOTCH signaling pathway involved in oocyte-GC crosstalk in follicogenesis.
932 The relative expression levels (log2 [FPKM+1]) of the specific ligands, receptors,
933 and target genes are shown. The diagrams at the left show the relationship among
934 these genes.
935 B) TGF-β signaling pathway involved in oocyte-GC crosstalk.
936 C) Gap junction involved in oocyte-GC crosstalk. The relative expression levels
937 (log2 [FPKM+1]) of the connexin genes are shown. The diagrams at the left show the
938 putative relationship among these genes.

939 **Figure 6. Comparison of Human and Mouse Oocyte Transcriptomic Profiles**
940 **during Folliculogenesis.**

941 A) Venn diagram of total expressed genes in human oocytes (peach) and mouse oocytes
942 (light green) demonstrates overlap between the gene populations in two species and
943 also overlap with the human housekeeping genes (deep orange). Pie chart represents
944 the non-housekeeping human-mouse oocyte-derived homologous genes (3,583),
945 including homologous DEGs (red) and homologous ubiquitous genes (green).
946 B) Heatmap of homologous DEGs in oocytes at five stages of folliculogenesis. The
947 numbers of identified DEGs are indicated on the y-axis, and the stages of follicle

948 development are presented along the x-axis. The color key from blue to red indicates
949 the relative gene expression level from low to high, respectively. The enriched GO
950 terms of human oocytes are shown on the right.
951 C) Bar plots demonstrate a comparative analysis of the selected oocyte-derived
952 homologous DEGs that show the distinct expression patterns in human (left) and mouse
953 (right) oocytes during folliculogenesis. Different colors represent different stages of
954 folliculogenesis.
955 D) Bar plots demonstrate a comparative analysis of four oocyte-derived homologous
956 DEGs that show the similar expression pattern in human (left) and mouse (right)
957 oocytes during folliculogenesis.
958 E) Bar plots demonstrate a comparative analysis of three homologous non-DEGs
959 annotated as oocyte maturation defect genes (OMIM) in human (left) and mouse (right)
960 oocytes during folliculogenesis.
961

962 **Supplementary Figure Legends**

963 **Figure S1. Sample Collection and Quality Control. Related to Figure 1 and 2.**

964 A) Table demonstrating number of samples per two follicle cell-type specific
965 compartments at five follicle stages.

966 B) Representation of the follicles in primordial, primary, secondary and antral stages.
967 Scale bar, 100 μm.

968 C) The number of detected genes (FPKM > 1) in each samples included in this study.

969 D) Saturation analysis for scRNA-Seq data. X-axis is mapped reads for each
970 down-sampling data, y-axis is number of genes detected.

971 E) Principal component analysis (PCA) of the transcriptome of human oocytes that
972 portrays sampling entities. Different colors and sizes of the points represent oocytes
973 of different stages and sizes, respectively. Different shapes of the points represent
974 different sampling entities (individuals).

975 **Figure S2. The Expression Patterns of Selected Marker Genes in Human**
976 **Oocytes and GCs. Related to Figure 2 and 3.**

977 A) Boxplots of selected marker genes in oocytes at each follicle stage.

978 B) Boxplots of selected hormone receptors and genes involved in steroidogenesis in
979 GCs at each follicle stage.

980 **Figure S3. The Expression Patterns of Signature Genes in Oocytes and GCs at**
981 **Each Stage. Related to Figure 2 and 3.**

982 A) Heatmap of signature genes in oocytes at five stages of folliculogenesis. The
983 numbers of identified signature genes are indicated on the y-axis, and the stages of

follicle development are presented along the x-axis. The color key from blue to red indicates the relative gene expression level from low to high, respectively.

B) Boxplots of the relative expression levels (log2 [FPKM+1]) of selected signature genes in oocytes to exemplify the expression patterns in each stage.

C) Heatmap of signature genes in GCs at different stages of folliculogenesis.

D) Boxplots of the relative expression levels (log2 [FPKM+1]) of selected signature genes in GCs to exemplify the expression patterns in each stage.

Figure S4. Secretory Protein Coding Signature Genes for Ovary Reserve Prediction.

A) Heatmap of the secretory protein encoding genes expressed in oocytes (left) and GCs (right). The list of these genes is indicated on the y-axis according to the five clusters by similarity of expression patterns, and the stages of follicle development are presented along the x-axis. The color key from blue to red indicates the relative gene expression level from low to high, respectively.

B) Boxplots of the relative expression levels (log2 [FPKM+1]) of selected secretory proteins encoding genes to exemplify the expression pattern in each cluster.

Figure S5. Inferred Key Transcriptional Factors in GCs at Each Stage-to-stage Transition of Folliculogenesis. Related to Figure 4.

A) MARINa plots of targets for each candidate master regulator. Red vertical bar represents the activated targets, blue represents the repressed targets. On the x axis, genes were rank-sorted according to the significance of differential expression between the two developmental stages. The candidate master regulators were

displayed on the right. The corresponding p-values of these master regulators indicate the significance of enrichment were displayed on the left.

B) Violin plots show the relative expression levels (log2 [FPKM+1]) of each master regulator in two consecutive stages.

Figure S6 Signaling Pathways Enriched in Follicle Recruitment and Antral Formation by GSEA/KEGG Analysis.

A) Heatmaps of DEGs between primordial and primary stage in oocytes and GCs. The numbers of identified DEGs are indicated on the y-axis, and the stages of follicle development are presented along the x-axis. The color key from blue to red indicates the relative gene expression level from low to high, respectively.

B) GSEA enrichment plots of KEGG signaling pathways in oocytes and GCs between primordial and primary stage.

C) Heatmaps of DEGs between secondary and antral stage in oocytes and GCs.

D) GSEA enrichment plots of KEGG signaling pathways in oocytes and GCs between secondary and antral stage.

Figure S7. The Expression of Putative Maternal-Effect Genes in Folliculogenesis and Early Embryonic Development.

A) Heatmap of the putative maternal-effect genes expressed in folliculogenesis and early embryonic development. The identified genes were clustered into four clusters by similarity of expression patterns. The stages of follicle development and early embryonic development are presented along the x-axis. Right panel show relative

1027 expression level of each cluster. The color key from blue to red indicates the relative

1028 gene expression level from low to high, respectively.

1029 B) Bar plots show the enriched GO terms of each cluster genes.

1030

Figure 1

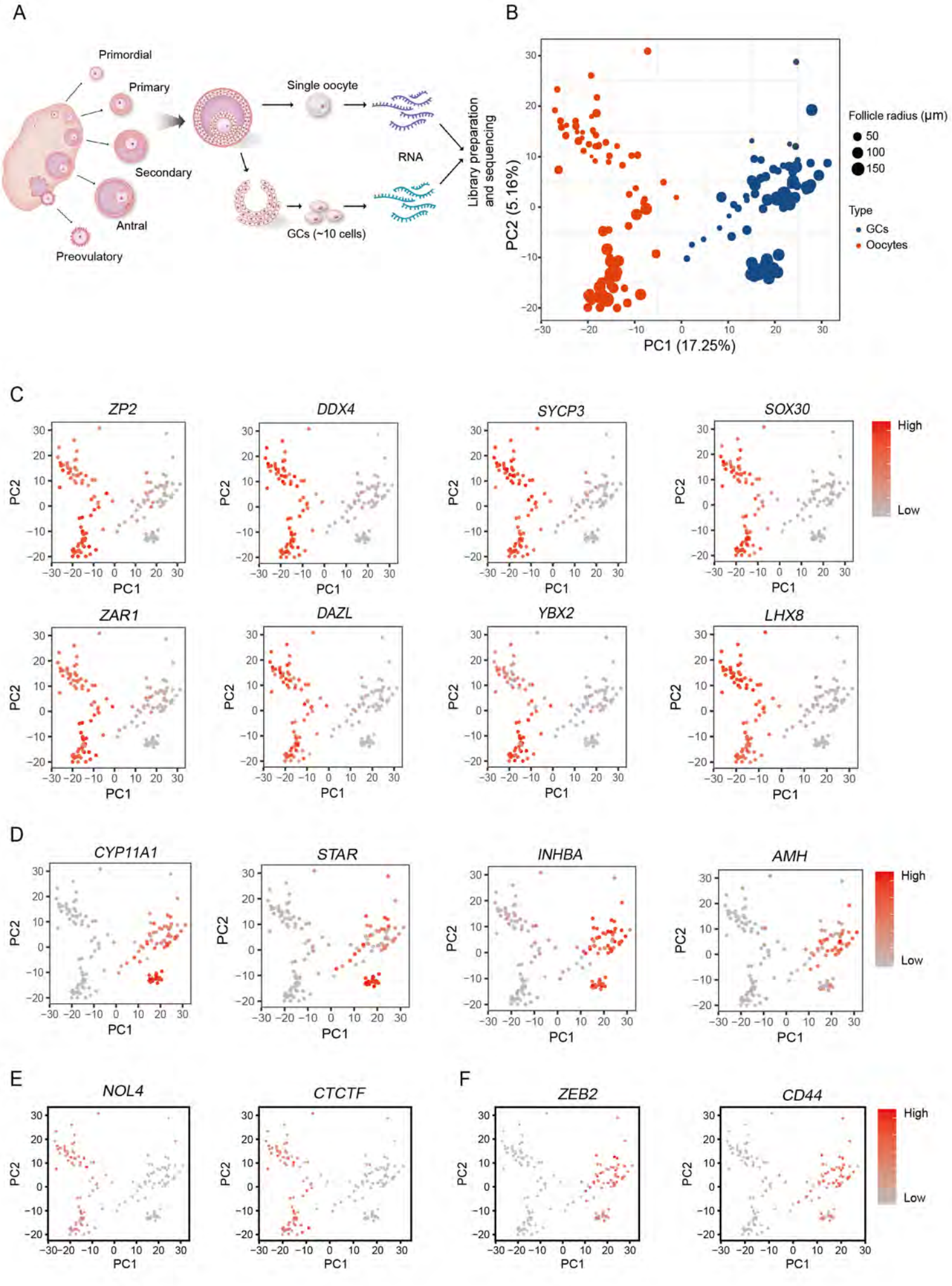

Figure 2

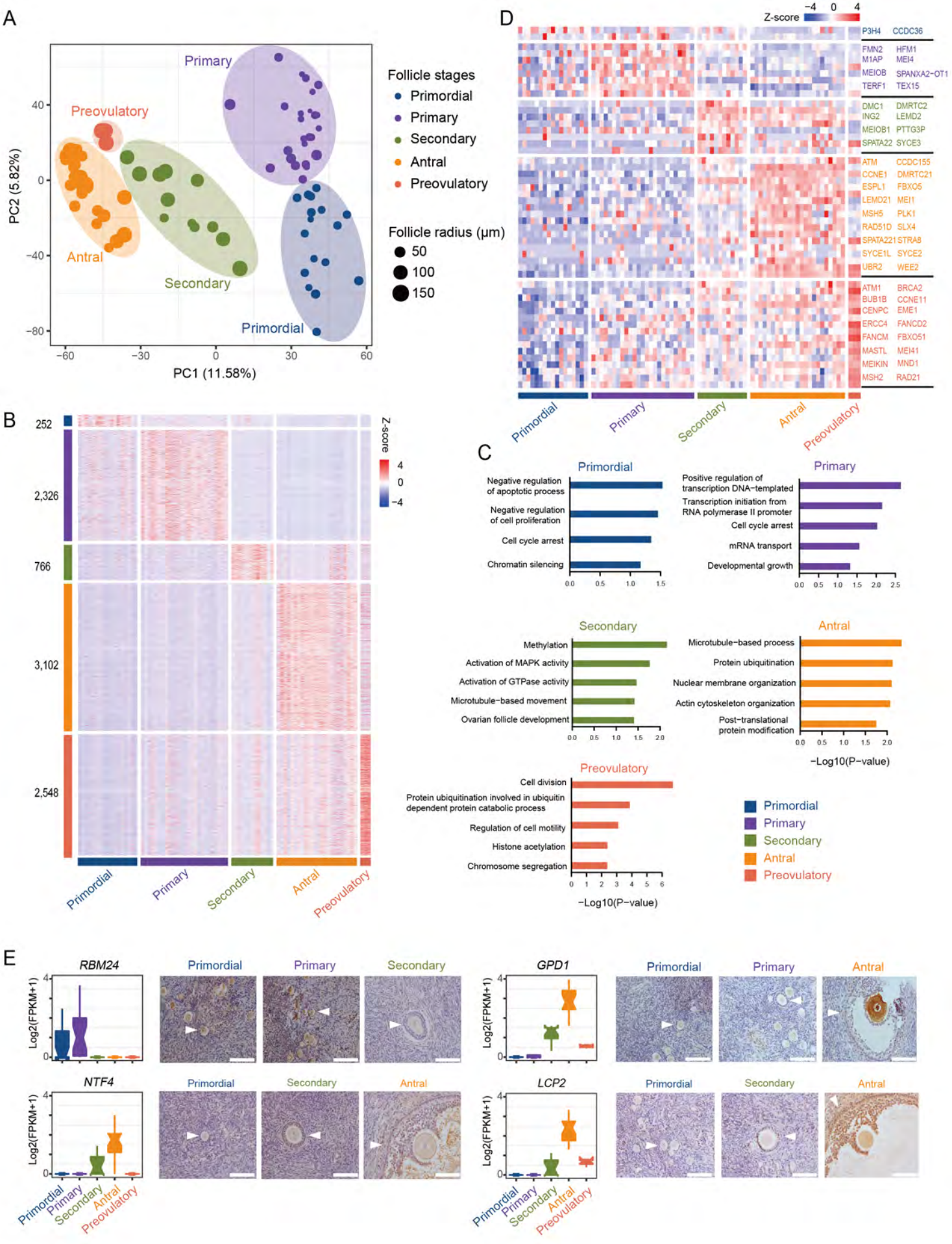

Figure 3

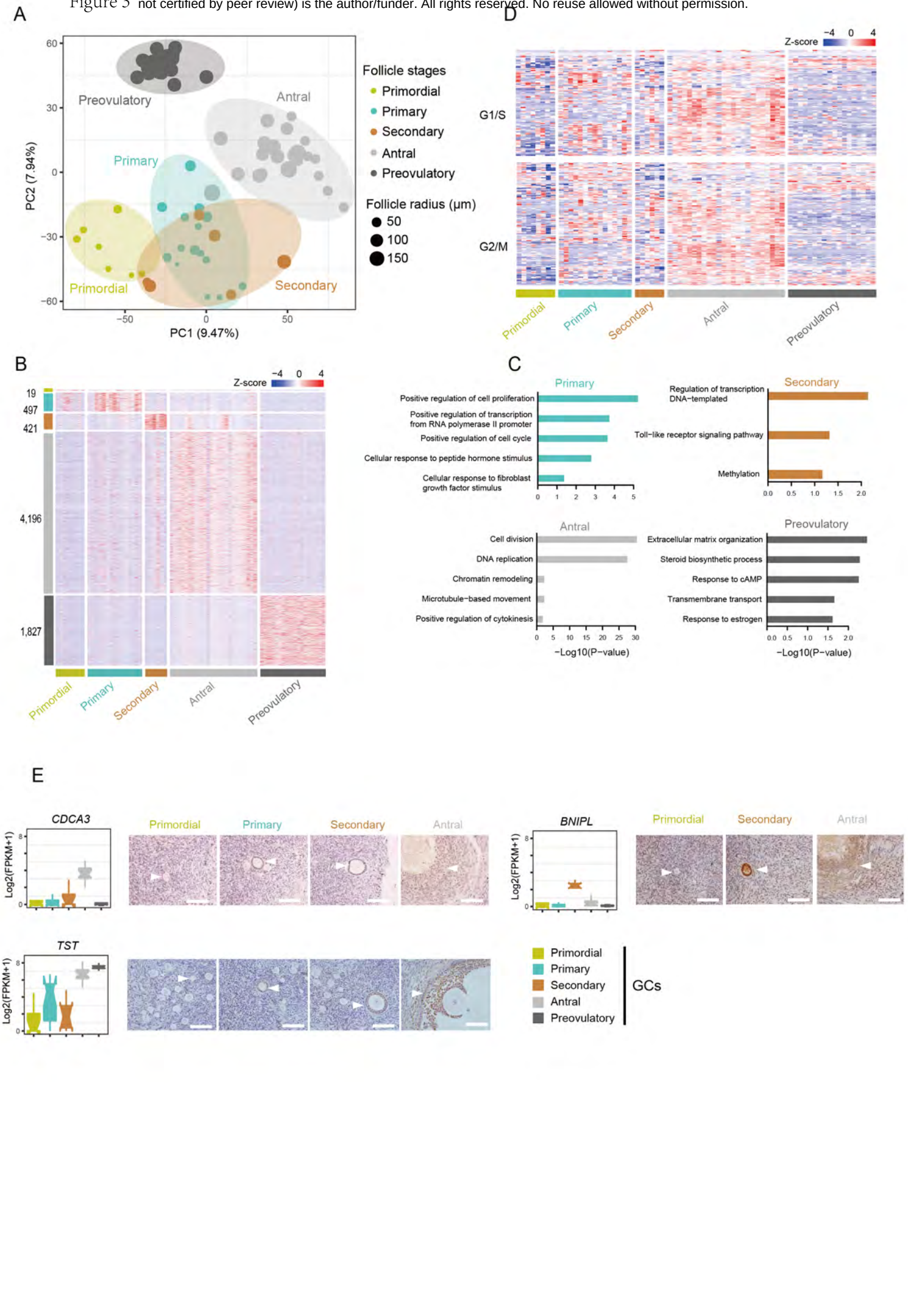

Figure 4

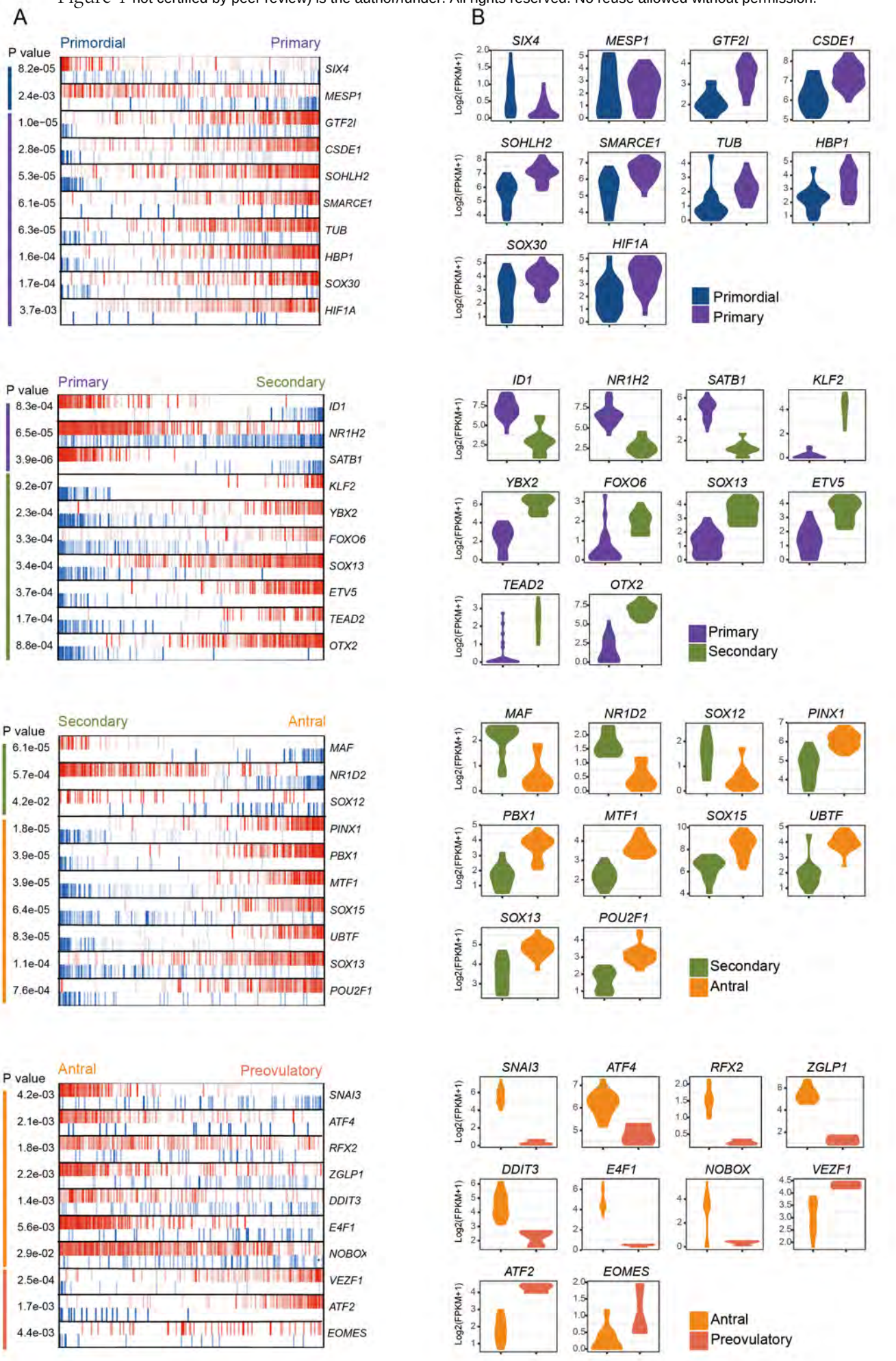

Figure 5

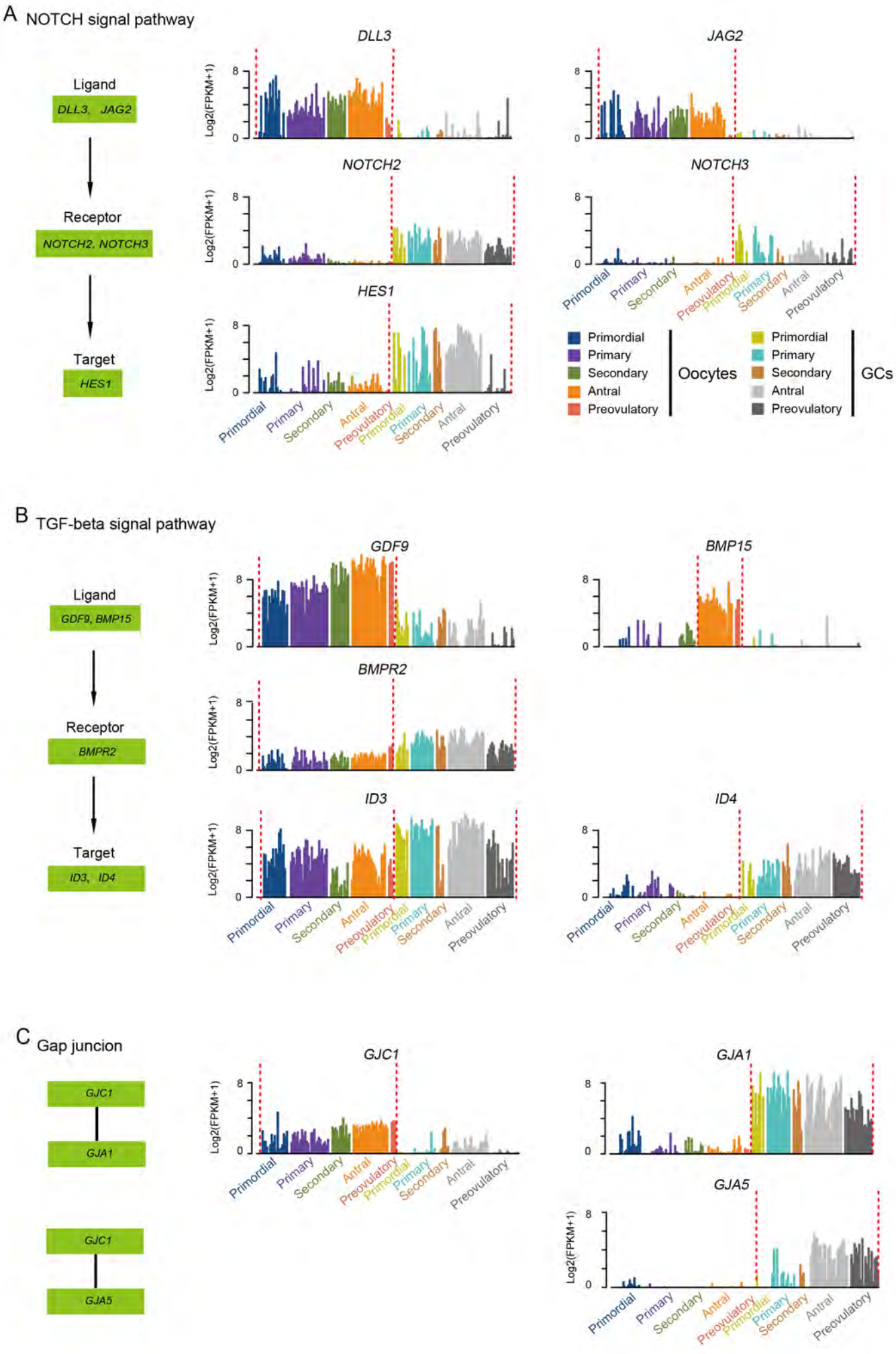

Figure 6

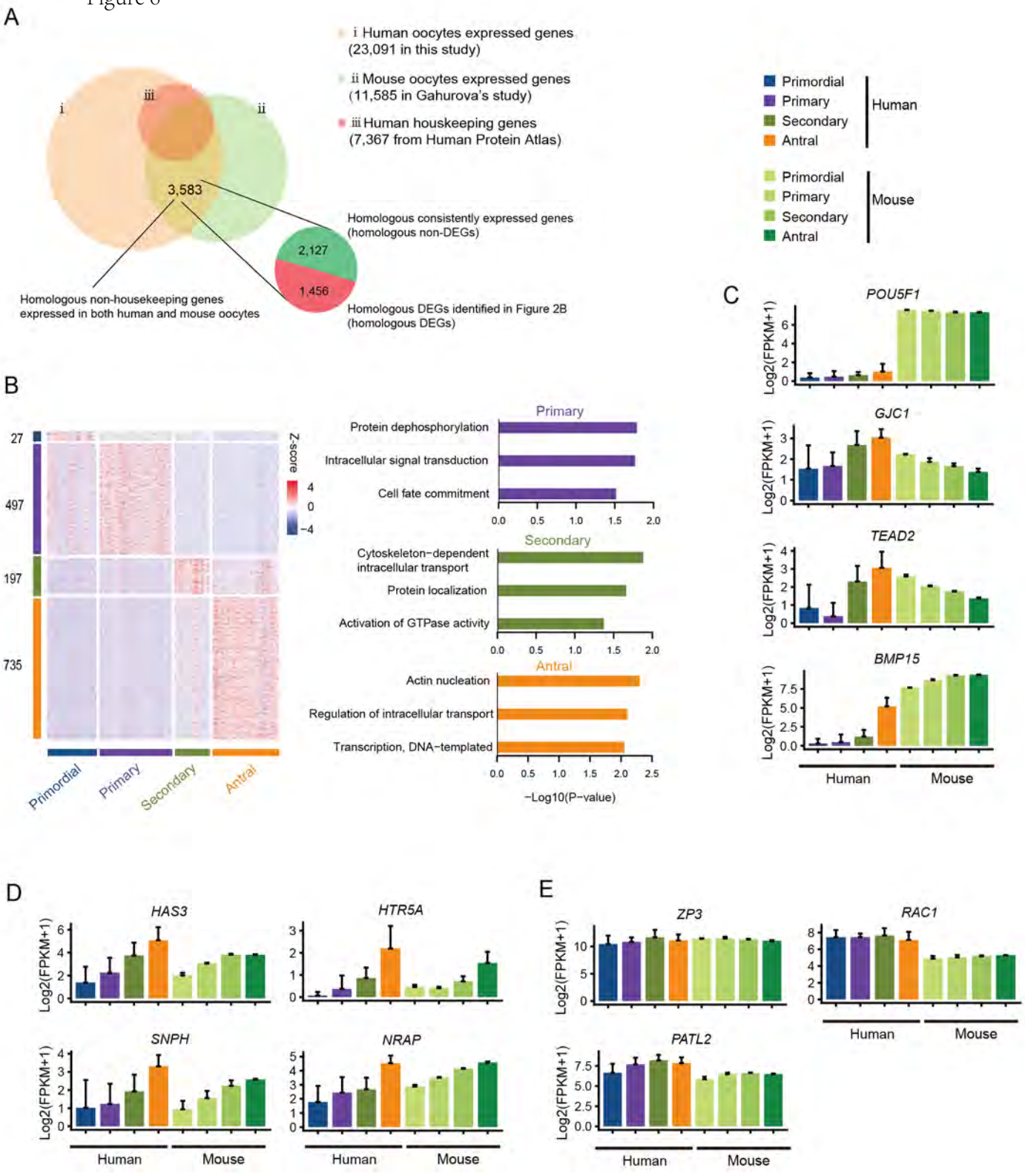

A

Follicle stages	Primordial	Primary	Secondary	Antral	Preovulatory	Total
Oocytes	17	25	12	23	3	80
GCs	8	15	6	24	18	71

B

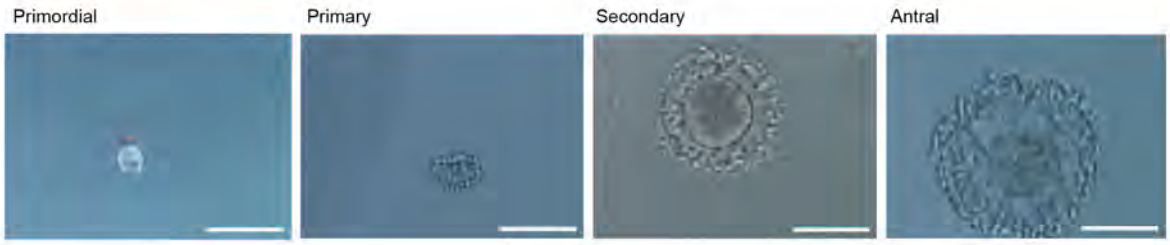

C

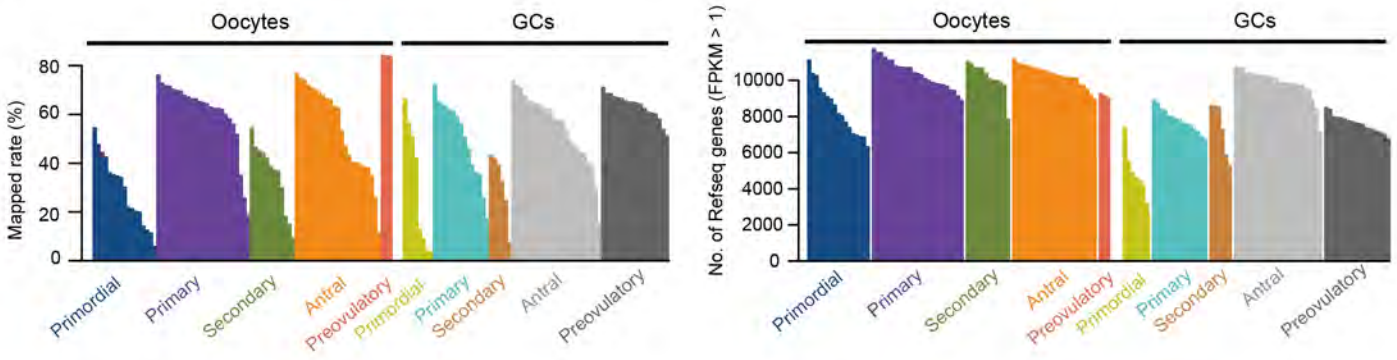

D

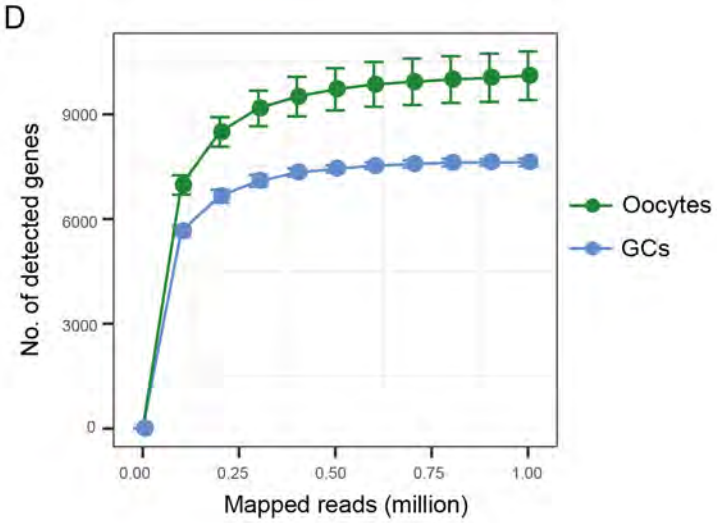

E

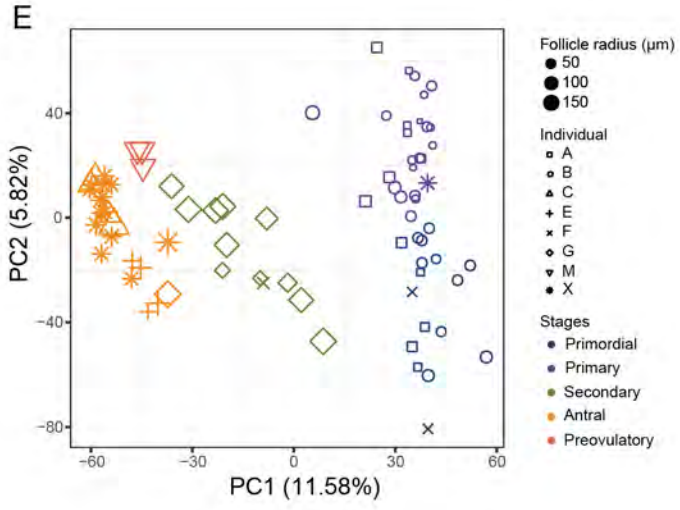

Extended Data Fig. 2a

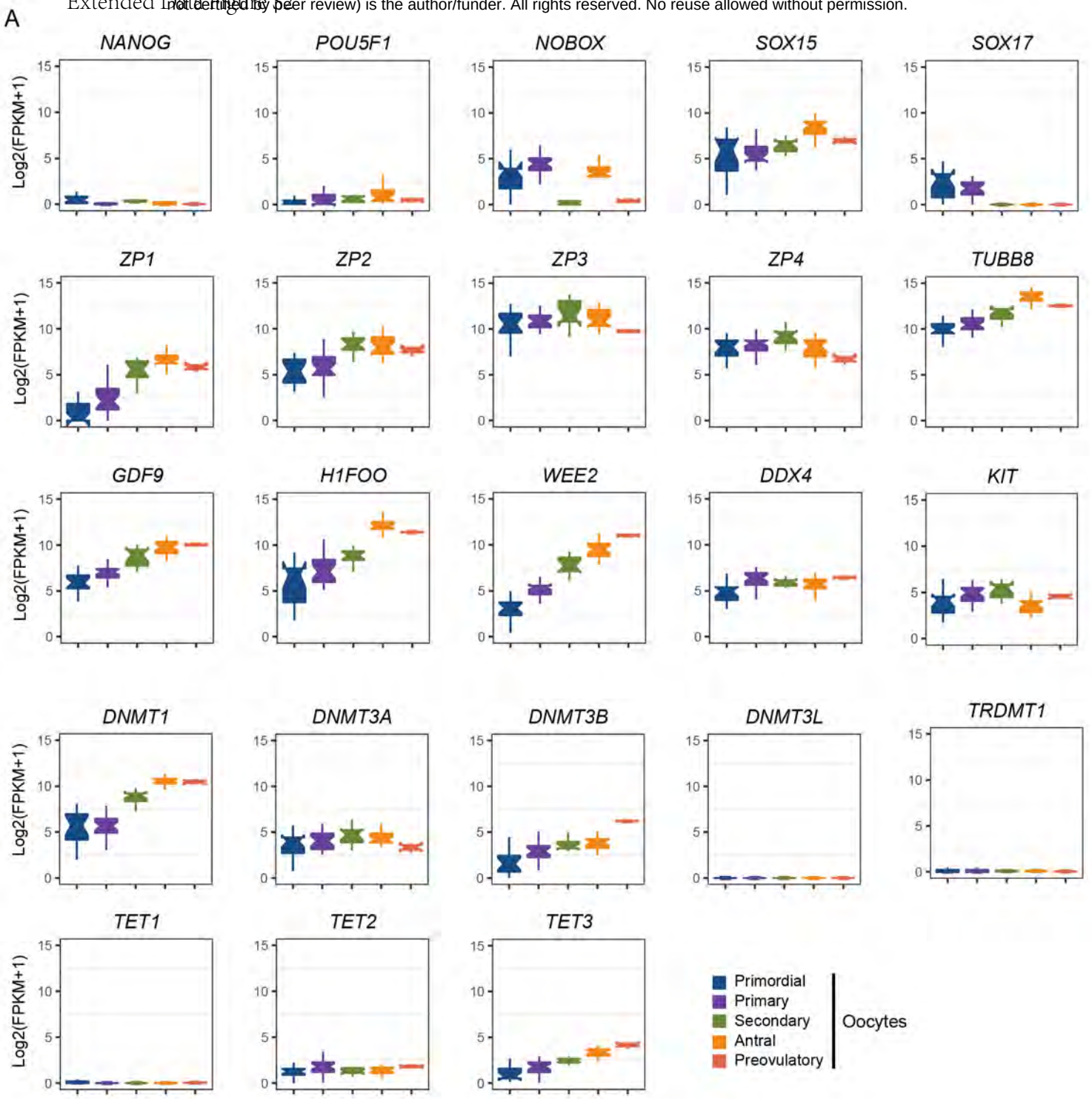

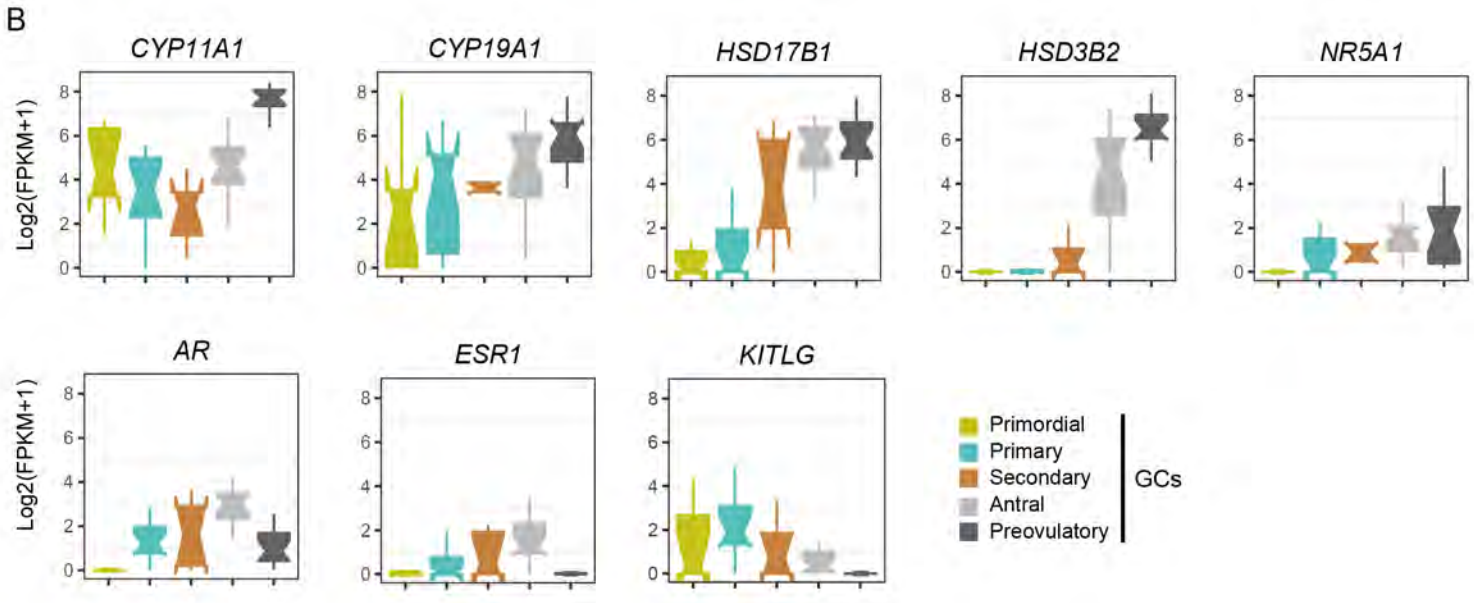

Extended Data Figure S3

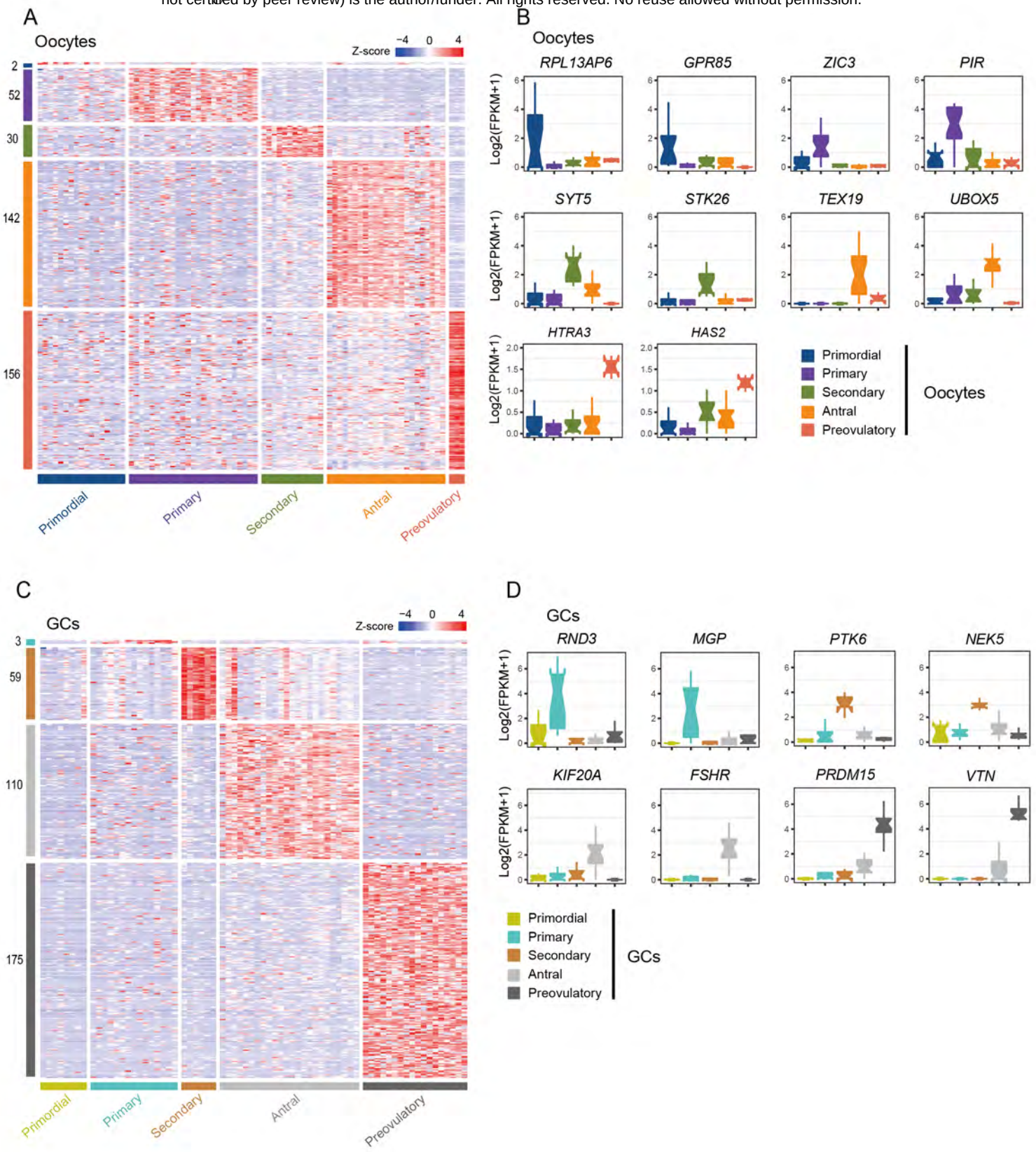

Extended Data Figure 3-4

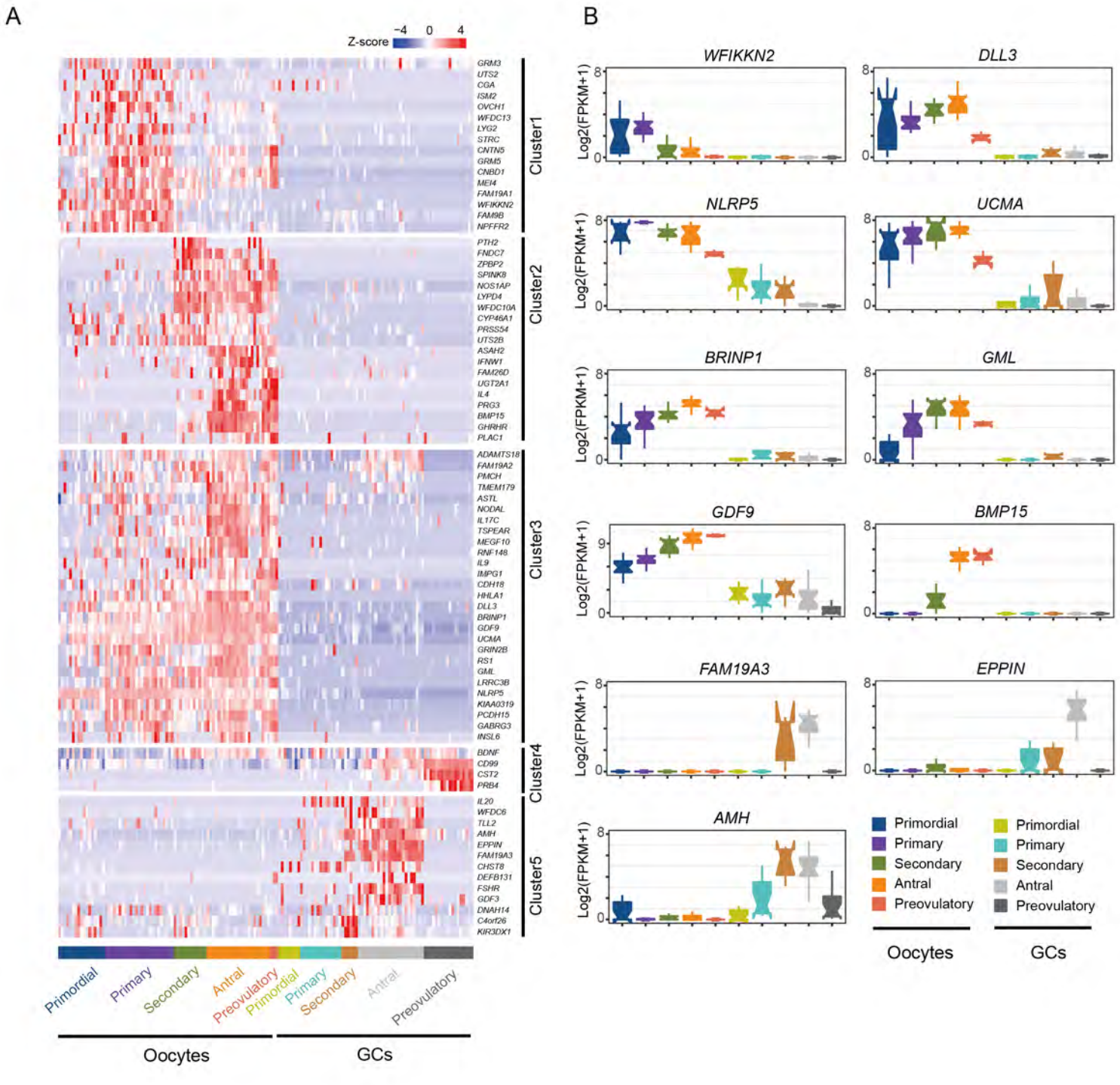

Extended Data Figure 3.